ESD-TDR-64-378

Technical Report 365

The Haystack Experimental Facility

H. G. Weiss

15 September 1964

Prepared under Electronic Systems Division Contract AF 19(628)-500 by

Lincoln Laboratory
MASSACHUSETTS INSTITUTE OF TECHNOLOGY
Lexington, Massachusetts

The work reported in this document was performed at Lincoln Laboratory, a center for research operated by Massachusetts Institute of Technology, with the support of the U.S. Air Force under Contract AF 19(628)-500.

MASSACHUSETTS INSTITUTE OF TECHNOLOGY

LINCOLN LABORATORY

THE HAYSTACK EXPERIMENTAL FACILITY

H. G. WEISS

Division 4

TECHNICAL REPORT 365

15 SEPTEMBER 1964

LEXINGTON MASSACHUSETTS

ABSTRACT

A new ground station for space communications, radar and radio astronomy research has recently been completed at Tyngsboro, Massachusetts. This installation, which is named Haystack, employs a 120-foot-diameter fully steerable antenna enclosed in a metal space-frame radome. Advanced design and construction techniques have been developed to achieve a reflector with a very precise parabolic contour. The antenna will operate very efficiently at wavelengths of 3 cm and will also provide a useful capability at wavelengths as short as 8 mm. The antenna incorporates a "plug-in" equipment room behind the reflector which makes it possible to conveniently utilize the antenna for a variety of both active and passive experiments. At the highest operating frequency, the half-power width of the antenna beam will be less than 0.02°. To provide appropriate control for this very narrow antenna beam, a general-purpose digital computer has been integrated into the facility. The RF configuration of the antenna is compatible with the use of high-power transmitters and cooled, low-noise receiving equipment. A versatile 1-Mw average power, high-voltage supply has been provided for energizing transmitting equipment. This new installation will provide a unique capability in the microwave portion of the spectrum for communications, radar and radio astronomy.

Accepted for the Air Force
Stanley J. Wisniewski
Lt Colonel, USAF
Chief, Lincoln Laboratory Office

TABLE OF CONTENTS

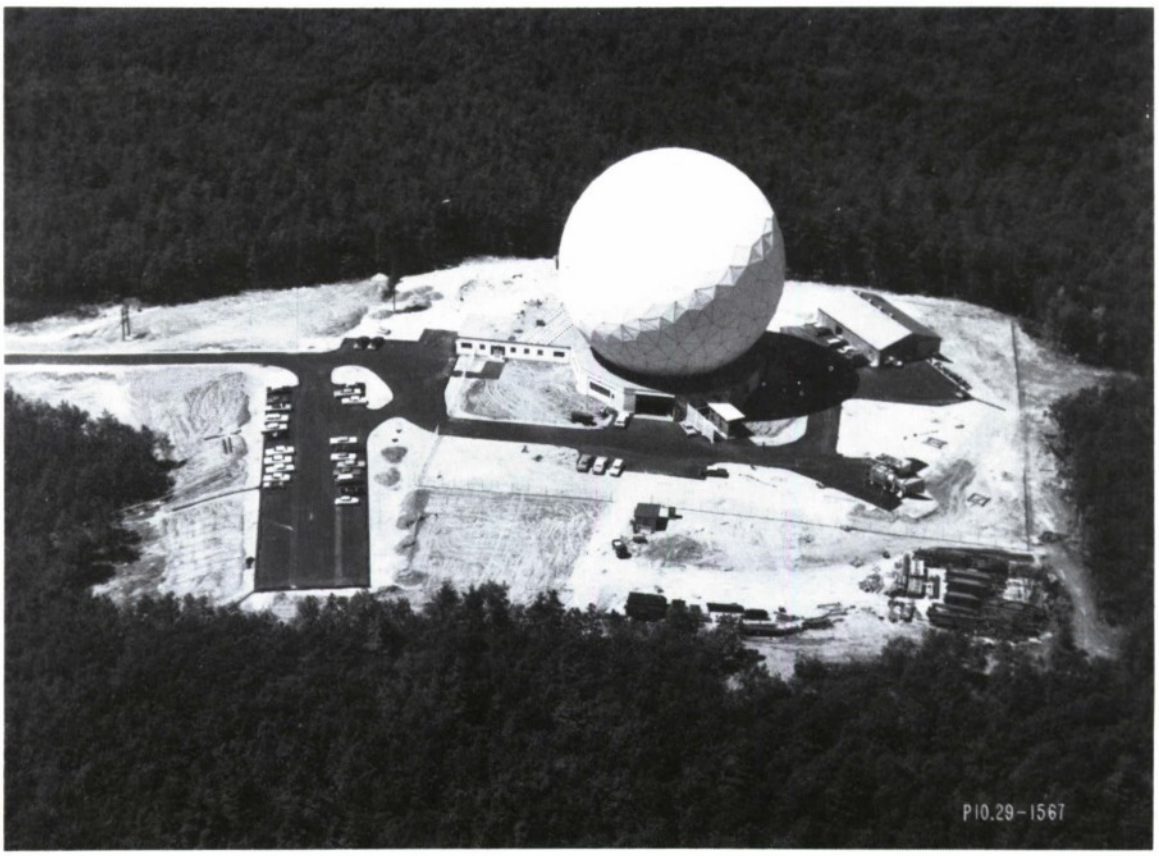

Fig. 1. Aerial photagraph af Haystack Experimental Facility.

THE HAYSTACK EXPERIMENTAL FACILITY

I. INTRODUCTION

For more than a decade, the M.I.T. Lincoln Laboratory has been conducting exploratory investigations in the fields of communications, radar, and radio physics. About five years ago, it became apparent that a new and more sensitive experimental facility would be required in the microwave portion of the radio spectrum to augment studies being conducted at longer wavelengths at the M.I.T. Millstone Hill Station in Westford, Massachusetts. The proposed investigations required a versatile installation capable of high-power transmission and low-noise reception in a variety of modes over the 1- to 35-Gcps frequency range. This report describes a new facility which has been recently established by the Lincoln Laboratory in Tyngsboro, Massachusetts, with support from the Electronic Systems Division of the U.S. Air Force. This new installation, which is commonly known by its code name, Haystack, is located approximately thirty miles northwest of Boston and about one-half mile from the Millstone Hill radar. A recent aerial photograph of the installation is shown in Fig. 1.

In 1958, only six months after the Millstone Hill UHF station became operational, the Lincoln Laboratory formally proposed to the Air Force that a very sensitive and versatile microwave experimental facility be constructed for communications and radar research. The research objectives proposed in 1958, in the fields of satellite communications, high-resolution radar, propagation research, and radar astronomy, still correspond closely to the activities which are now about to be undertaken at this new installation. The performance of the completed Haystack facility, however, exceeds the most ambitious early objectives in many respects. For example, a Lincoln Laboratory engineering report of July 1958 stated that the desired system should have an antenna surface tolerance of 0.175 inch rms, with maximum local deviation not to exceed 0.375 inch. The report cautioned that the achievement of these tolerances would require a "departure from standard fabrication techniques," since they called for an accuracy some ten times greater than was "generally considered to be tight control" at that time. The completed antenna has an rms surface error of less than 0.025 inch and a maximum deviation of only 0.075 inch – approximately 7 times more accurate than the early objective. This precision has extended the useful range of the antenna to at least 35 Gcps.

Comparable improvements have been realized throughout the rest of the system. The mechanical and electrical design features provide a system with unprecedented sensitivity, versatility, frequency coverage, and flexibility of operation. Equally significant is the integration of a high-speed, general-purpose, digital computer into the system to provide for pointing, tracking, and presenting both raw and processed results to the user, who is thereby largely freed from many tedious and error-prone manipulations. The installation can readily be converted to operate

in any one of a variety of modes throughout the 1-Gcps to 35-Gcps frequency range, and will have unique capabilities for space communications, radio astronomy and long-range radar tracking experiments.

Some of the more significant aspects of the Haystack program are listed below.

(a) Improved techniques have been developed for analyzing complex mechanical structures. As a result of this program, it is now possible to predict the behavior of complex space-frame and shell structures with an uncertainty of about one part in 100,000. This is about two orders of magnitude more precise than could be accomplished by using the design techniques available at the start of this program.

(b) By the integration of a "plug-in" equipment room within the antenna structure, and by the development of a versatile cabling system, it will be possible to employ the system efficiently for many different applications. In addition, this "plug-in" equipment concept will permit the system capability to be updated easily as improved electronic components become available.

(c) The use of a digital computer in the antenna control system in real time enables an unskilled operator to utilize the antenna in an efficient and flexible manner. In addition, the use of the computer to record and reduce experimental data in real time increases the sensitivity and flexibility of the installation.

(d) An RF configuration has been employed which permits the efficient use of low-noise receivers and high-power microwave transmitters. This capability, plus the high precision of the antenna surface and pointing system, will provide high system sensitivity in a microwave portion of the spectrum for long-range communications and radar tracking experiments.

(e) A metal space-frame radome is employed for the first time in a low-noise microwave system. Radomes of this type are of interest since they can be constructed in much larger sizes and provide good electrical performance over a wide frequency range.

(f) An unusual hydrostatic bearing has been developed which permits the positioning and control of massive structures with great precision. This class of bearing has low static friction and should be essentially free from wear.

II. ANTENNA

A. Performance Requirements

Because of the wide variety of proposed uses for the Haystack antenna, the specification of its operating frequency range was somewhat arbitrary. There were several specific radar and communication studies which required the use of a large aperture antenna at a wavelength of

3 cm, and other scientific programs of interest to the Laboratory could make effective use of a large antenna at considerably shorter wavelengths. The longest nominal operating wavelength was chosen to be 30 cm in order to permit the antenna to be used for hydrogen-line and L-band radar studies. To be of practical value for the proposed communications and radar studies, the antenna efficiency would have to remain high for all pointing angles and throughout the range of environmental conditions that would be encountered in a New England site.

It became evident early in the program that it would be unrealistic to undertake the development of a large precision microwave antenna unless it were protected from the New England environment. As discussed in Sec. III, the availability of a 150-foot-diameter radome influenced the decision to limit the diameter of the antenna to 120 feet, since this was the largest antenna on an azimuth-elevation mount which could be housed within this radome.

To achieve an antenna with efficient performance at the higher end of the microwave spectrum, a performance goal was selected which required an aperture efficiency only 0.3 db below that obtainable from an ideal 120-foot-diameter parabolic reflector at a wavelength of 3 cm. The fulfillment of this requirement would permit the antenna to be useful at wavelengths as short as 8 mm. The attainment of this performance objective would represent a significant advance over previous antenna designs and would make the development program technically challenging.

The relationship between the surface tolerance of a reflector antenna and its aperture efficiency at several wavelengths is plotted in Fig. 2. To meet the specified performance criterion, the reflector surface should not deviate more than 0.025 λ (rms) from an ideal reflector. For λ = 3 cm, this corresponds to ±0.075 cm. In working with production drawings, manufacturing operations, and field measurement practices, it is more convenient to specify peak tolerances rather than rms tolerances, and since experience has shown that the peak surface deviation of a typical antenna is approximately 2.5 times its rms deviation, the ±0.075-cm rms tolerance corresponds to a peak value of ±0.187 cm, or about ±0.075 inch. Therefore, the antenna specification was written to require that all points on the reflector surface remain within ±0.075 inch (peak-to-peak) from the ideal parabolic contour under the anticipated operating conditions. This allowable peak error of 0.075 inch must include all surface errors resulting from gravity forces (varying with rotation), thermal effects, manufacturing errors, and field erection and calibration errors.

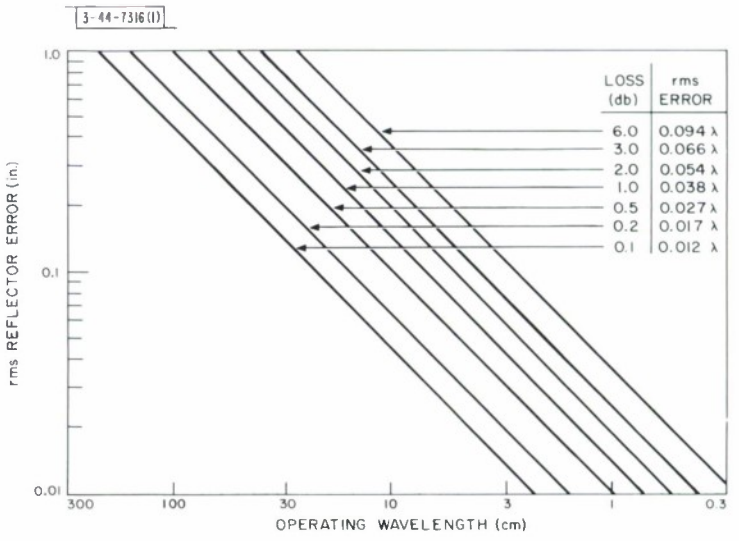

Fig. 2. Loss due to reflector toleronce (from J. Ruze equotion).

To meet this requirement, design and measurement techniques would have to be developed which would contribute an uncertainty of perhaps only 0.02 inch maximum. In a 120-foot-diameter structure, this corresponds to about one part in 70,000 and represents a substantially more stringent design requirement than has been achieved in any large movable structure to date. In recent years, several programs to construct large steerable antennas did not meet with full success. Therefore, it seemed particularly important to demonstrate that much of the risk could be eliminated in the design of large steerable antennas by proper planning and by an adequate design and engineering effort. Perhaps one of the most important lessons of the Haystack program has been the reaffirmation of the value of a methodical scientific approach in the design of new antenna systems.

A 120-foot-diameter antenna at a frequency of 10 Gcps will produce a radiation pattern with a main lobe width that is 0.05° between 3-db response points. To utilize this narrow beam effectively, it is necessary to direct the beam position in celestial coordinates with an error that is only a small fraction of a beamwidth. For this reason, the specifications were written to require that the pointing error not exceed 0.005° (18 arc seconds) at slow tracking rates. While the tracking rates that would be encountered in most experiments would be relatively slow, it was anticipated that there would be occasions when it would be desirable to transfer from one object in the sky to another in a relatively brief period. For this reason, it was specified that the antenna be able to move from one pointing position to any arbitrary pointing position in the hemisphere and achieve a maximum pointing error of 0.005° in less than 60 seconds.

It was recognized that it would be difficult, if not impossible, to utilize efficiently an antenna with this narrow a beam without some form of pointing computer. Because of the variety of experiments to be performed with the antenna, it seemed advisable to integrate a general-purpose digital computer into the pointing control system. The use of an appropriate computer in this manner would enable the antenna to be directed from data obtained over telephone or radio circuits from a remote location, and rapid and accurate parallax and time-delay corrections could be introduced. The use of the computer would also enable semiautomatic compensation to be achieved for systematic pointing errors that might result from displacement of the feed with elevation motion, lack of orthogonality in the elevation and azimuth axes, systematic errors in the shaft encoder, etc. It would provide the possibility of introducing corrections for the refractive index of the atmosphere, which would be significant at elevation angles below 15°.

A Cassegrainian reflector system was selected because it combined good electromagnetic performance with a basic configuration that permitted the placement of electronic components near the center of gravity of the moving structure. The energy spillover from the primary feed horn of a Cassegrainian antenna is largely in the direction of the "cold" sky, and this is a desirable attribute for a low-temperature antenna. The size of the hyperbolic secondary reflector is chosen to be 9 feet, 4 inches in diameter so that, at the lowest nominal wavelength – namely, 30 cm – the size of the secondary reflector would equal that of the feed.

To provide a convenient way for carrying out a variety of experiments with the antenna, the concept of interchangeable "plug-in" instrumentation rooms was evolved. These plug-in rooms, mounted immediately behind the primary reflector surface, would contain low-noise receivers, radio-frequency transmitter components, and antenna feed systems. The Cassegrainian geometry adopted for this antenna in conjunction with the plug-in room concept permits the use of low-noise receivers and high-power microwave transmitters, and requires only short waveguide

runs without rotary joints. The plug-in room was specified to be 8 feet × 8 feet × 12 feet in size and to have a maximum gross weight of 7000 pounds. An integral hoist system was to be incorporated into the antenna structure to facilitate the interchanging of plug-in rooms. Power, water, and other services would be conveyed to the equipment by cables with quick-disconnect plugs. The characteristics of the antenna are summarized in Fig. 3.

B. Development Approach

After the characteristics of the antenna system were established, performance specifications were prepared, and design proposals were solicited from fourteen commercial organizations. Many of the industrial firms that submitted design proposals had considerable experience with conventional antennas, but a study of these proposals revealed that an adequate engineering basis for designing an antenna to fulfill the stated performance objectives did not exist. The techniques then available for estimating the performance of an antenna required that the structure be approximated by a greatly simplified two-dimensional mathematical model, and study revealed that these simplifying assumptions would make it impossible to obtain a valid analysis of any complex, moving structure which was accurate to better than about one part in about 300.

Therefore, the original specifications were modified to include development of a comprehensive analytic computer program to confirm the validity of any proposed design, the construction and testing of a 1/15 scale structural model and the comparison of the performance of this model with that predicted by the computer program, preassembly of the complete antenna system at the contractor's plant, and then proof-loading and checking against predicted performance prior to shipment to the site. A further stipulation in the contract called for the submission of all drawings to Lincoln Laboratory for approval prior to release to production.

C. Description of Antenna Configuration

In December 1960, a contract was awarded by the Air Force to the North American Aviation, Inc. Columbus (Ohio) Division for the design, construction, and installation of the Haystack antenna system. The basic structural configuration proposed by NAA is shown in Figs. 4 and 5. It consists of a reflector backup structure comprised of five concentric tubular ring trusses interconnected by pretensioned diagonal rods. The main supporting ring, which is 60 feet in diameter, is bridged by two trunnion trusses that are attached to the main ring at its quadrant points and carry its load to the elevation bearings. Two ring trusses are positioned outboard of the main support ring, and two smaller ring trusses are positioned inboard of the main ring. The pretensioned interconnection rods are designed to work without stress reversals as the antenna rotates. In the trunnion beams and the support rings, where high compression loads occur, and where some stress reversals cannot be avoided, heavy-wall large-diameter tubing was used, and considerable effort was expended in the development of a bolted joint that was not susceptible to creep. This configuration results in a structure that is unusually stiff in proportion to its weight.

The reflector surface, which is supported from the backup structure by means of adjustable standoff studs, is made up of 32 inner panels and 64 outer panels. These panels consist of thin aluminum prestretched skins, 0.016 inch thick, bonded to a $\frac{1}{2}$-inch-thick aluminum honeycomb core. The panels are interlocked by shear keys. Adjustable expanders are located at 2-foot intervals along the radial edges of each panel to determine the gap between panels. One circumferential edge of each inner and outer panel is firmly attached to a 60-foot-diameter annular

Perfarmance Gools

Aperture efficiency within 0.3 db of on ideal reflector ot 10 Gcps.

A pointing system compotible with the 0.05° half-power beamwidth.

Pointing rotes odequote to trock low-oltitude sotellites.

Cossegroinian Reflector System

	Parabalic	Hyperbolic
Diameter	120 ft	9-1/3 ft
Focol length	48 ft	
Surface toleronce peok porallel to oxis of symmetry	±0.075 in.	±0.005 in.

Positioning Perfomonce

	Precision	Intermediote	Slew
Moximum position error	±0.005 deg	±0.0125 deg	None
Moximum velocity	1.0 deg/sec	2.5 deg/sec	3.3 deg/sec
Moximum occelerotion	0.012 deg/sec^2	0.03 deg/sec^2	As required

Shoft Angle Data Systems

Digital	19-bit parallel binary with ±1-bit accurocy (±0.0007°)
Synchra	400 cycle, 1 speed (±0.1° accurocy)

Mechonicol

RF plug-in room	8 × 8 × 12 ft, 7000 lb
Reflector surfoce	
Porobolic	96 honeycomb panels, solid skin
Hyperbolic	Single honeycomb panel, solid skin
Azimuth-elevation drives	Dual ontibocklosh, gear troins, valve servo
Azimuth bearings	Full hydrostotic, 16 thrust and 8 radiol pads
Elevatian beorings	Dual spherical self-aligning roller
Antenno weights	
On elevation axis	196,900 lb
On ozimuth oxis	376,000 lb

Operoting Environment

Temperoture range	0° to 110°F
Solor radiation	6% of rodiotion incident on rodame
Wind velocity in rodome	Zera

Fig. 3. Chorocteristics of Hoystock ontenno.

Fig. 4. 1/15 scale model of Haystack antenna.

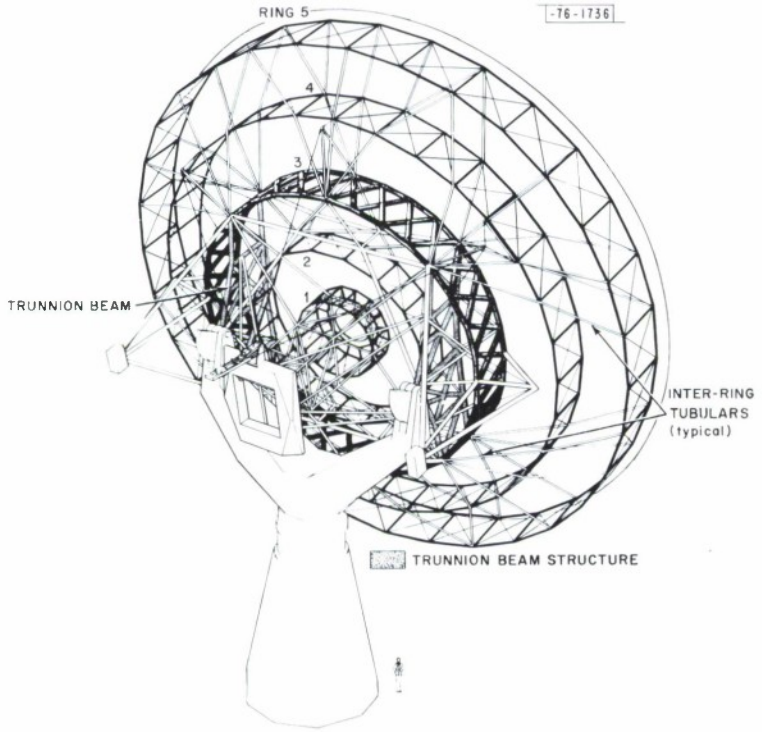

Fig. 5. Basic structural configuration of Haystack antenna.

ring, which in turn is supported from adjustable standoffs from the main ring. Each panel is also attached to two of the other ring trusses by adjustable standoffs which are placed normal to the local contour. These have ball and socket joints at each end and thus take only axial loading.

The 96 individual reflector panels are made to behave like a homogeneous shell by the use of 26 concentric circumferential cables located behind the reflector surface (Fig. 6). These pretensioned cables, which act like large "elastic bands," are guided by adjustable rollers mounted on the back of the reflector panels, close to the panel surface. The exact contour of the reflector surface can be adjusted by the interpanel expanders, the adjustable standoffs at the rings, and the spacing between the cable rollers and the back of the panel. By forcing the individual panels to work as a homogeneous shell, the stiffness of the reflector surface is increased about tenfold, and the relatively lightweight reflector surface contributes significantly to the over-all rigidity of the complete antenna system. When the reflector is rotated away from the vertical, the integral shell is restrained from lateral movement relative to the backup structure by 32 shear pins that are installed between the shell and the trunnion trusses.

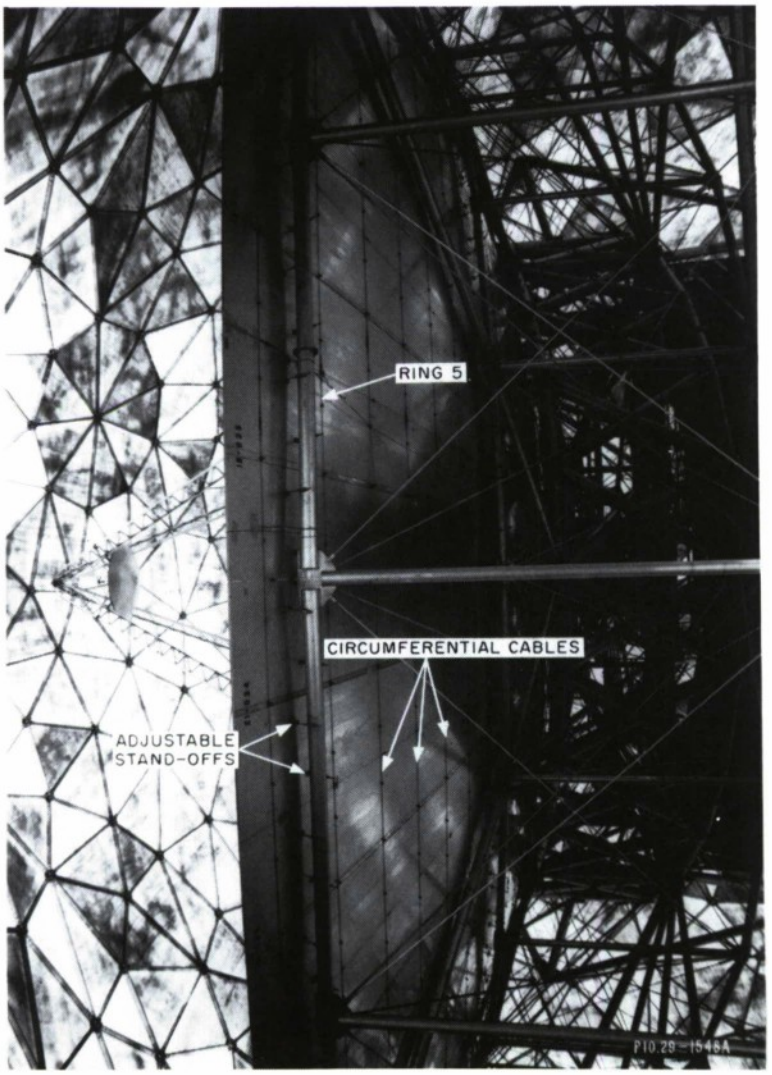

Fig. 6. Side view of antenna.

The Cassegrainian secondary reflector is a 9-foot, 4-inch-diameter hyperbolic surface supported by a planar truss quadripod. The reflector size was selected to permit operation at wavelengths as low as 1 Gcps. The quadripod legs are attached to the main ring at the trunnion beam "hard" points and each truss is guyed by four pretensioned rods. The reflector surface was explosively formed from a 0.188-inch-thick sheet of aluminum which was then bonded to a 2-inch-thick honeycomb stiffener. The front surface of the aluminum sheet was then milled in a digital controlled boring mill. While the hyperbolic reflector axis was established in the boring mill, an optical flat, 2 inches in diameter, was carefully located at the center of the hyperbolic reflector with its axis coincident with the reflector axis to within 1 second of arc. In this manner, a relatively lightweight but very rigid precision secondary surface was obtained. The surface of the secondary reflector has a tolerance of ±0.005 inch. The position and tilt angle of the secondary reflector are adjustable by lead screw actuators which are remotely controlled.

D. Quality Control and Measurement System

Great care has been taken in the design and production of the reflector panels (Fig. 7). Refined measurement and quality control techniques had to be developed by NAA to produce panels that would conform to the theoretical contour with an rms deviation of approximately 0.010 inch when measured in a precision test fixture in a temperature-controlled environment. These panels, which are nearly 30 feet long, were fabricated on a precision, doubly curved mold and employed a thermal-setting epoxy to bond the prestretched aluminum skins to the honeycomb core. The panels were then placed in a precision drill and trim fixture, still in a constant-temperature room, where they were trimmed and sixteen optical targets carefully located on

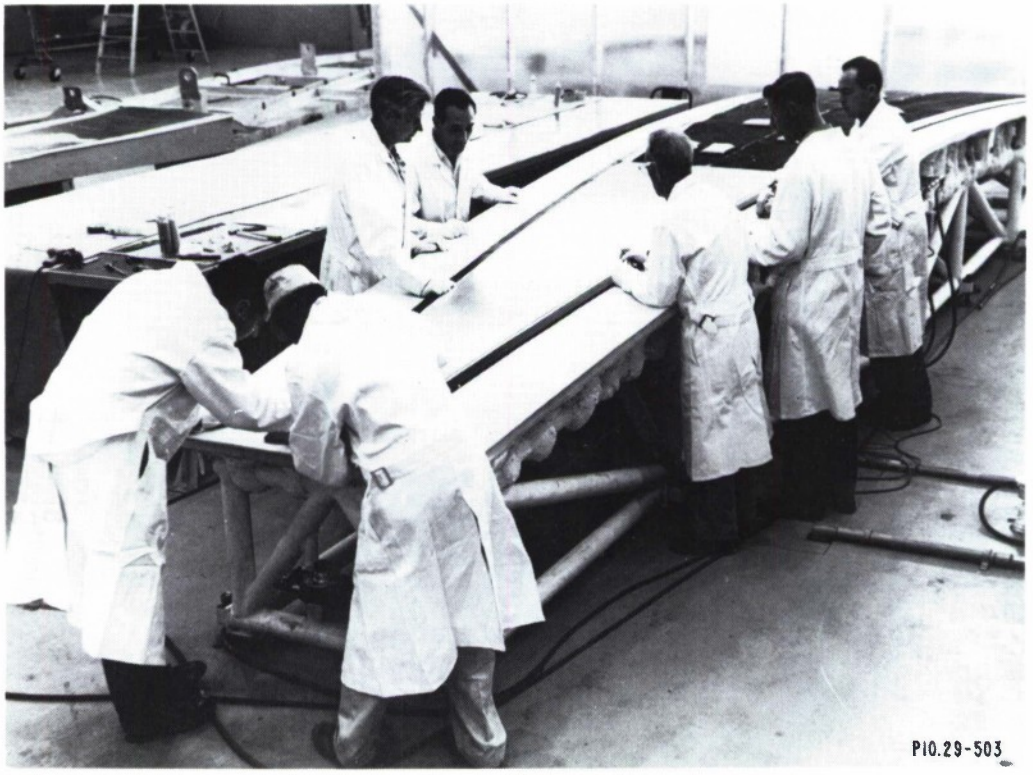

Fig. 7. Reflector panel fabrication.

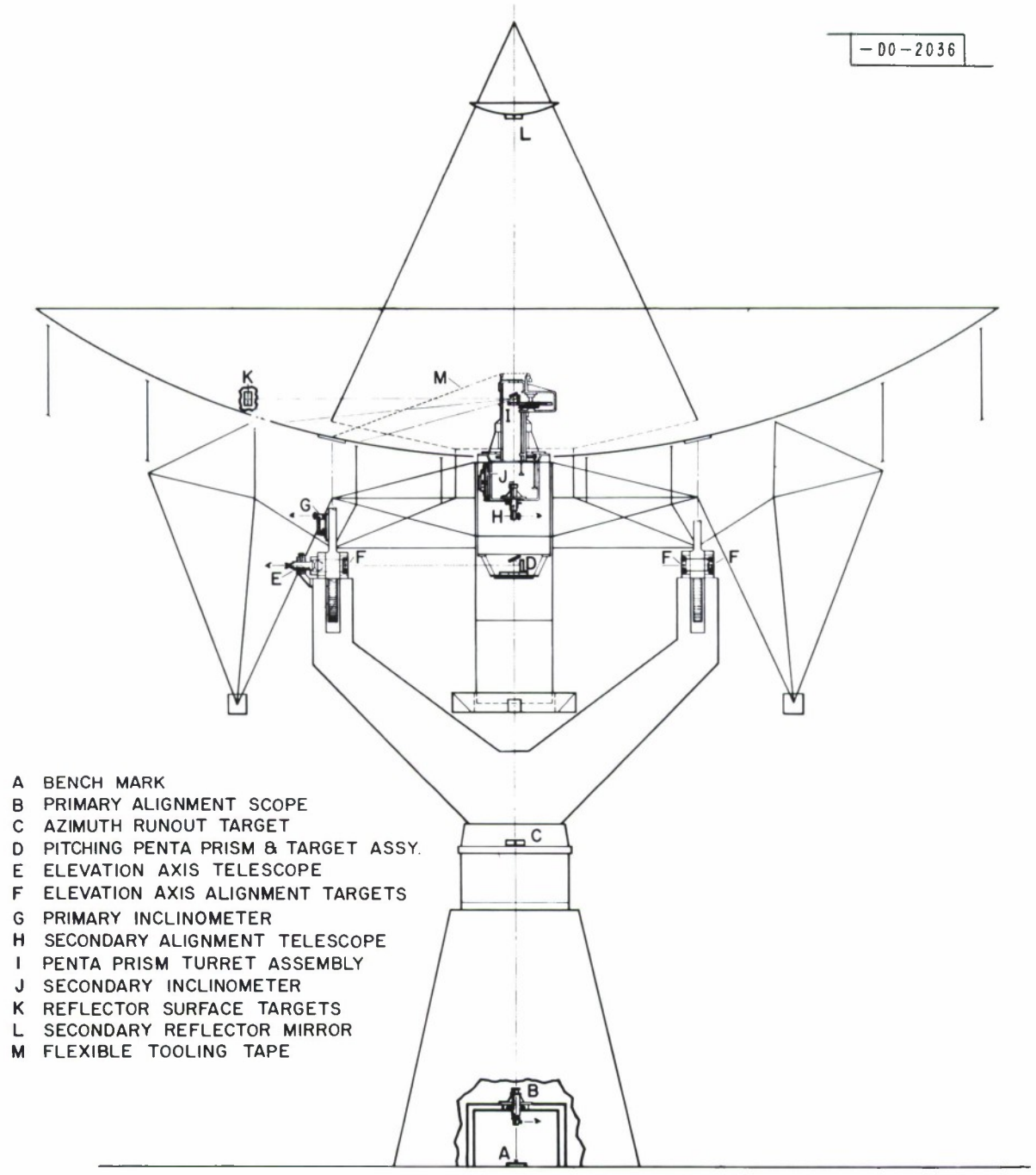

Fig. 8. Optical alignment system.

each reflector panel surface. The tolerance in locating these targets within any given panel is 0.003 inch.

After the antenna has been assembled, the surface is adjusted by the use of the system of optical elements shown schematically in Fig. 8. The optical system consists primarily of alignment telescopes, precision levels, ruled circles, targets, pentamirrors, and a calibrated tape. Each element is the most precise unit of its kind available. To facilitate the use of the alignment system, the over-all antenna configuration has been designed to preserve optical paths from the ground through the azimuth and elevation axes.

The primary optical probe for adjusting the surface contour was built by Keuffel & Esser Company of Hoboken, New Jersey under subcontract from North American Aviation. This probe (Fig. 9) is mounted in a plug-in room, which has its center of gravity and total weight matched to that of a typical plug-in equipment room. A special chair on gimbals has been provided to permit an observer to use the optical probe while the antenna is rotated in elevation. The upper head of the calibration probe may be rotated and contains eight indexable, fixed-angle pentamirrors that permit observation of eight circular rows of targets on the reflector surface. Each pentamirror, which has been calibrated to have an error of less than 1 second of arc, rotates the line of sight the proper amount to view a circle of targets on the reflector surface. This system does not require an outside reference, and it permits referencing all target points with respect to four "hard points" located where the secondary reflector quadripod legs join the main support ring. Experience in using the optical probe at the Haystack site has indicated that, when the thermal environment is relatively stable (at night), the repeatability of the optical measurements on a day-to-day basis is within 2 seconds of arc. This corresponds to an uncertainty of about 0.007 inch in a direction normal to the line of sight at a radius of 60 feet.

E. Bearing and Control System

The bearings used for the elevation and azimuth axes of the antenna are of two distinctly different types. In the azimuth axis, an externally pressurized oil-film bearing is employed (Fig. 10). The lower portion of this bearing consists of a 6-foot-high load distribution cylinder which is located between the rotating portion of the antenna and the concrete tower. The azimuth bull gear, which is about 14 feet in diameter, is bolted to this distribution cylinder and serves as a support ring for the hydrostatic bearing pads. These pads, each of which has an effective surface of 8×14 inches, are attached to the support ring by bolts. Sixteen pads are used for the thrust bearing, and eight pads are used for the radial bearing. The combined weight of the pad, ring, and structural member is 42,000 pounds. Adjustable wedge block assemblies are used between the concrete tower and the load distribution cylinder to permit releveling of the bearing.

The upper load distribution ring is approximately 14 feet in diameter and 4 feet high. The ring, which weighs approximately 24,000 pounds, contains integral thrust and radial runner surfaces that have been flame-hardened and surface-ground. It is a very stiff weldment, which has been designed to distribute the concentrated loads that are conveyed from the yoke arms. The bearing pads operate with an oil-film thickness of approximately 0.005 inch. A temperature-compensated flow-control valve has been inserted between the pump, which is common to all pads in the bearing, and each bearing pad in order to isolate the downstream effect from the

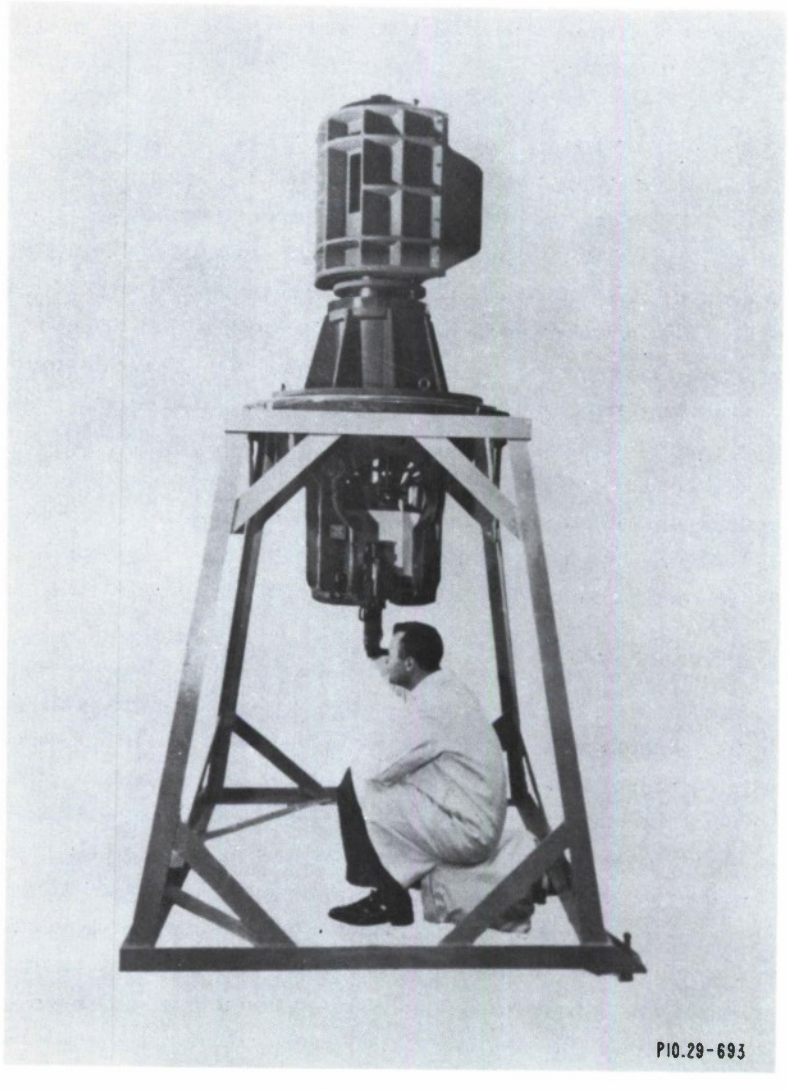

Fig. 9. Optical probe.

HYDRAULIC DRIVE

POWER TRAIN			TACH DRIVE		
GEAR	NO TEETH	G.R.	GEAR	NO TEETH	G.R.
1	21	.266	7	96	4.57
2	79		8	21	
3	21	.250	9	105	4.38
4	84		10	24	
5	26	.046			
BULL	564				

DATA BOX DRIVE

CAM DRIVE			SYNCHRO DRIVE		
GEAR	NO TEETH	G.R.	GEAR	NO TEETH	G.R.
BULL	564	21.7	BULL	564	21.7
1	26		1	26	
2	30	.250	2	30	.250
3	120		3	120	
4	28	.199	4	28	.199
6	141		5	141	
7	64	.500	4	28	.199
8	128		6	141	

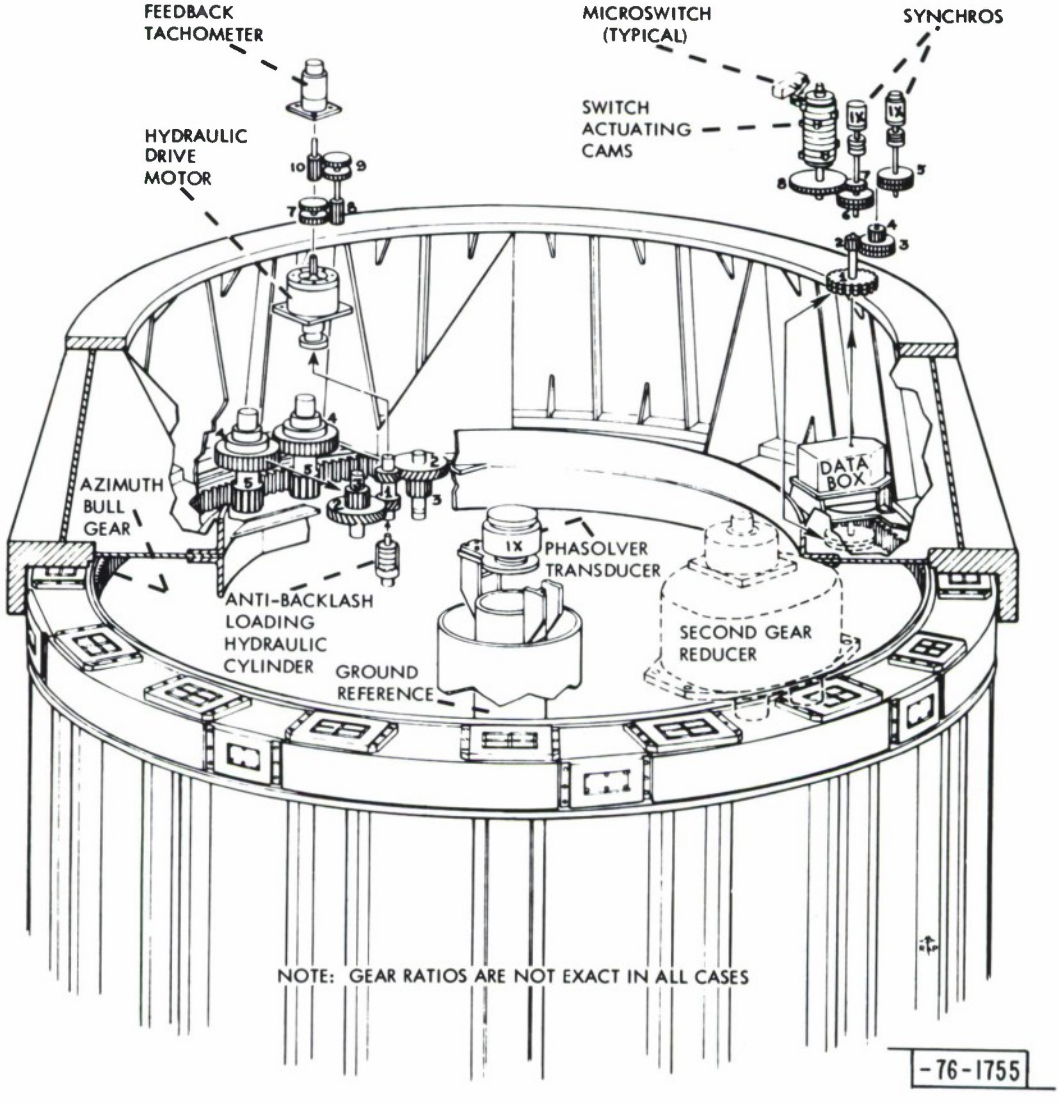

Fig. 10. Azimuth bearing and gear train.

other bearing pads. The normal operating pool pressure is 250 psi, and an oil flow of approximately 26 gallons per minute is required for both thrust and radial bearings. This type of bearing should provide extremely smooth performance and have long life.

Conventional self-aligning, spherical, roller bearing assemblies are used in the elevation axis. Because the diameter of the elevation bearings is relatively small (10.5 inches), the "stiction" torques are of very small magnitude. An oil circulation system is used to force-lubricate these bearings. The alignment of the bearing pads on the top of the yoke arms is accomplished by the use of positioning brackets and by shims under the pillow blocks. An optical path has been provided along the bearing axis to facilitate their alignment.

To insure that the antenna will not rotate beyond the nominal travel limits, a self-contained oil-air buffer stop has been provided. The buffers are of the linear type, somewhat similar to those used in aircraft landing systems. The buffer systems have been designed to decelerate the antenna safely when it is moving with full drive torque and with maximum velocity.

The azimuth and elevation antenna drive elements each employ two hydraulic motors and gear-reducer systems. Dual pinnion drives contact the bull gear at each gear box and use two parallel gear trains hydromechanically loaded to minimize backlash. The hydraulic servo motor, which has a 20-horsepower rating, employs a series of radially placed pistons that push against a multilobe cam to make it rotate. This type of motor has extremely smooth low-speed characteristics.

The Haystack antenna has two angle-data systems. One system is a conventional one-speed synchro-loop and provides a reduced accuracy standby position control for checkout operations and emergency control. The accuracy of the synchro readout system is $\pm 0.1°$. The more precise digital control and data system was specifically developed for the Haystack antenna. A shaft-angle transducer consisting of two electrostatically coupled, 8-inch-diameter glass discs has been developed by the Telecomputing Corporation, LaMesa, California, for the program. One disc revolves on its own bearings and is coupled directly to the antenna shaft, rotating with the antenna at one speed; the other disc is fixed to the encoder housing. Clearance between discs is approximately 0.003 inch. One disc contains three sets of conductive patterns consisting of paired 90° displaced sine waves. This electrostatic resolver provides 256 fine-electrical-phase vector rotations and 8 medium-phase vector rotations for one antenna shaft revolution. Quantizing electronics converts the electrical phase information into pulse form for use in a counter-comparator. The least significant bit of the precision shaft encoder corresponds to 2.47 seconds of arc. Specially designed shaft couplers are employed to allow small alignment errors between the encoder shaft and the moving antenna without causing angular errors.

F. Analytic and Test Program

In 1957, the Department of Civil Engineering at M.I.T. under the sponsorship of Lincoln Laboratory developed a computer program for use in structural analysis of large space truss structures. This program, capable of handling up to 60 joints, was modified and expanded to the extent that by 1960 a program was available that could analyze space structures with up to 4000 joints. The acronym, STAIR (STructural Analysis Interpretive Routine), was adopted for this program. The basic parameters of STAIR as programmed for Haystack on the IBM 7094 are indicated in Fig. 11.

Basically, STAIR considers the Haystack backup structure as comprised of truss members with pin-ended joints, but with no provisions made for member bending or torsion, or for moment

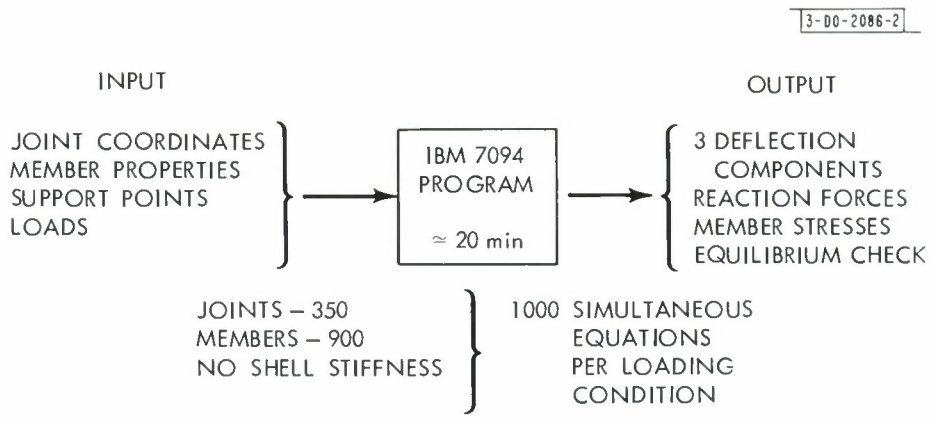

Fig. 11. STAIR program.

transfer at the joints. A unique feature of STAIR is the method of preparing the input, which consists of dividing the joints into groups which are called "units." For each unit a stiffness matrix is calculated, each element of which represents the resistance to displacement of a joint in the direction of one of the principal orthogonal axes. Successive steps of matrix addition and reduction are then carried out until the entire structure finally is represented in a single matrix. The final matrix is inverted and multiplied by the applied load matrix to obtain joint deflections. Deflections of the joints previously eliminated are obtained by back substitution. The program then calculates the force in each member from the deflections of its ends. An important feature of the program is a final status check, in which the forces at each joint are summed and tested for equilibrium.

With STAIR available in 1960, Lincoln Laboratory was able to check independently the analytical work submitted by North American Aviation. The original two-dimensional hand calculations on the backup structure performed by NAA were not verified by STAIR. The analysis was in error by an order of magnitude (hand prediction 0.010 inch vs STAIR prediction 0.110 inch). STAIR, by virtue of its ability to look at local surface areas, was able to identify specific design deficiencies. The hand analysis could not do this, since it provides only maximum deflection data on an area basis and does not give point-by-point distortion information. This is an important distinction, since the Haystack reflector panel contour is deliberately distorted when it is adjusted in a face-up attitude, to minimize surface errors when the antenna is oriented to an attitude of 45 degrees.

A 1/15 scale structural test model was constructed and tested for deflections under various loading conditions. STAIR was utilized to predict the model deflections with the applied loads in various tests. Correlation of model and computer results fell within 15 to 20 percent. This provided the first opportunity to establish the validity of the STAIR program.

By mid-1961, NAA had completed an independent analysis, using a separate NAA-generated computer program. There was excellent correlation between deflections computed by STAIR and NAA. Of the values tabulated, 93 percent agree within 0.001 inch, and the largest difference was 0.018 inch, at a point where the deflections had a value of 0.241 inch. It became quite evident with the agreement of both programs that redesign of the backup structure was necessary, since the deflections were not within specification. The NAA program was now utilized as a design

BACK-UP STRUCTURE DEFLECTION COMPARISONS
IN-PLANT TESTS – BACK-UP STRUCTURE ONLY
RF DIRECTION DEFLECTIONS (in.)
(For Target and Load Locations See Fig. 13)

3-40-7734

LOAD DIRECTION	TEST	LOAD	RESULTS FROM / NODE POINT (Target Raw and Number)	H-1	H-7	H-9	H-17 H-49 (avg)	H-33	F-1	F-17
FACE-UP TYPE LOAD	1	2000 lb H-1 and H-33	TEST	−0.265	−0.052	0.042	0.081	−0.234	−0.102	0.050
			COMP. NAA	−0.223	−0.054	0.040	0.088	−0.223	−0.102	0.053
			COMP. STAIR	−0.223	−0.054	0.040	0.088	−0.241	−0.101	0.053
			COMP. FRAN	−0.223	−0.051	0.037	0.082	−0.232	−0.095	0.049
	2	2000 lb H-17 and H-49	TEST	0.066	0.039	−0.025	−0.363	0.075	0.049	−0.099
			COMP. NAA	0.076	0.045	−0.033	−0.343	0.076	0.053	−0.104
			COMP. STAIR	0.076	0.046	−0.033	−0.345	0.078	0.053	−0.104
			COMP. FRAN	0.070	0.043	−0.029	−0.333	0.071	0.047	−0.097
	3	1000 lb H-9, H-25, H-41 and H-57	TEST	−0.012	−0.033	−0.032	0.009	−0.006	−0.003	0.007
			COMP. NAA	−0.005	−0.037	−0.037	0.009	−0.005	−0.002	0.002
			COMP. STAIR	−0.005	−0.037	−0.036	0.010	−0.004	−0.002	0.003
			COMP. FRAN	−0.006	−0.037	−0.035	0.011	−0.005	−0.003	0.003
FACE-SIDE TYPE LOAD	4	2000 lb H-1 and H-33	TEST	−0.040	−0.009	0.000	0.003	0.043	−0.017	0.000
			COMP. NAA	−0.041	−0.009	0.002	0.000	0.041	−0.017	0.000
			COMP. STAIR	−0.041	−0.009	0.003	0.000	0.051	−0.017	0.000
			COMP. FRAN	−0.040	−0.009	0.002	0.001	0.049	−0.016	0.001
	5	2000 lb H-17 and H-49	TEST	−0.015	−0.004	0.002	−0.003	0.012	−0.008	0.000
			COMP. NAA	−0.015	−0.011	0.000	0.000	0.015	−0.010	0.000
			COMP. STAIR	−0.015	−0.010	0.001	0.001	0.016	−0.009	0.000
			COMP. FRAN	−0.014	−0.010	0.001	0.001	0.015	−0.009	0.001
	6	1000 lb H-9, H-25, H-41 and H-57	TEST	−0.001	−0.004	−0.017	−0.001	0.008	0.001	−0.003
			COMP. NAA	−0.008	−0.011	−0.019	0.000	0.008	−0.005	0.000
			COMP. STAIR	−0.007	−0.010	−0.018	0.000	0.008	−0.004	0.000
			COMP. FRAN	−0.007	−0.010	−0.018	0.001	0.007	−0.005	−0.001

Fig. 12. Camparisan between calculated and measured deflectians.

tool and was employed to analyze about 40 antenna configurations with up to 30 loading conditions each. After five months of analysis, modifications to the backup structure were established that would reduce the deflections to meet the specifications. Computer time totaled approximately 150 hours on an IBM 704, and about 7000 man-hours of support and evaluation were used. Meanwhile, in the same period at Lincoln Laboratory, 50 hours of IBM 7090 time were expended in STAIR runs on 10 to 15 configurations with up to 10 loading conditions per configuration. Approximately 2000 man-hours supported this effort. At the conclusion of this phase of the project, results of both computer programs indicated that it would be possible to predict the deflections of the reflector within ±0.005 inch. The maximum deflection due to gravity from face-up to face-side, as computed by NAA and checked by STAIR, was ±0.040 inch, which was a reasonable value for gravity effects.

To minimize reflector distortion due to thermal effects, all parts of the reflector system were made of one material – namely, aluminum. For design studies, the vertical temperature gradient of the air within the radome was estimated to be approximately 10 °F and, in addition, the temperature of the air near the side of the radome facing the sun was estimated to be about 10 °F above that of the air near the opposite side. The effect of these gradients on the structure was studied using the Lincoln STAIR program. These studies predicted that surface distortions as large as ±0.017 inch would occur with a 10 °F gradient across the radome diameter. Later experience has shown that the estimate for the temperate gradient could be exceeded on hot sunny days; therefore, an air-moving system has been incorporated into the radome.

In December 1962, when the actual backup structure had been fabricated and assembled at the NAA plant, a series of static load tests was carried out. The structural assembly, at the time of the in-plant tests during December 1962, included the entire basic ring structure, the trunnion beams, and the RF raceway structure. Portions of the antenna, which were omitted in the assembly, were also left out of the analysis, so that the analytical structure was as close as possible to the actual test structure. The items not included in these tests were the honeycomb surface panels, the quadripod support structure for the secondary reflector, and the tri-ballast counterweight structure along with its associated pendulum ballast beams and cables. Six separate load configurations were applied to the structure, and deflections were measured at preselected points throughout the structure. The tests consisted of loading a small number of joints on the structure with weights applied through cables. There were three cases with loads applied vertically, as in the face-up position, and three cases with loads applied horizontally. After reducing raw data to eliminate rigid body rotation and translation of the structure, resulting deflections were compared with both STAIR and NAA computed deflections for the same loading conditions. Figure 12 lists the tests and comparable computed deflections for the x-direction (parallel to the reflector focal axis) loads as analyzed by both Lincoln Laboratory (STAIR and FRAN) and NAA. The reference coordinate system employed is shown in Fig. 13.

Considering that the accuracy of the reduced test deflection data was about ±0.010 inch, a study of the tables reveals good correlation between measured and computer-predicted results. Ninety-four percent of all the measured test deflections were no more than 0.010 inch away from the STAIR-computed values, and 69 per cent were no more than 0.005 inch from computed values.

A third computer program, developed in the intervening time by IBM, was also used to calculate deflections. This program is called FRAN, an acronym for FRame ANalysis. The Haystack antenna was one of the initial test problems run on the FRAN program.

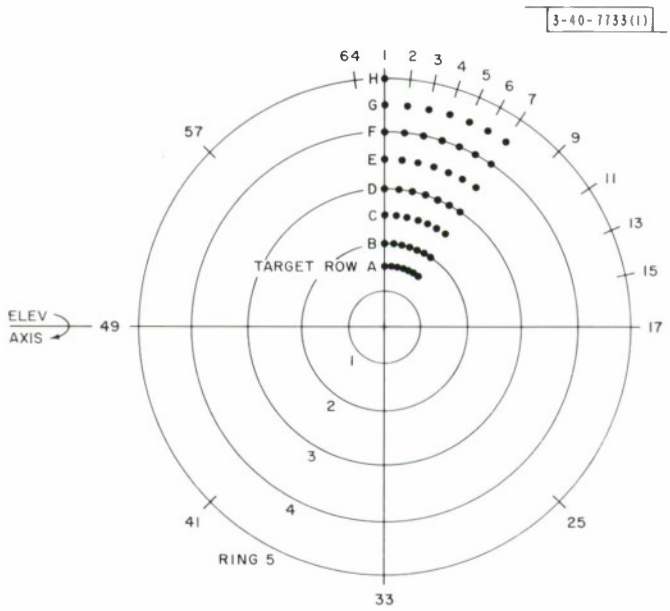

Fig. 13. Reference coordinate system.

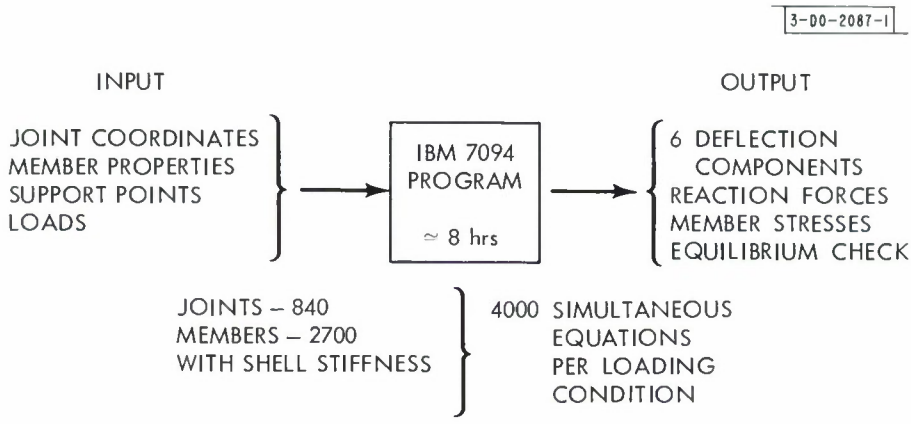

Fig. 14. FRAN program.

Over the past year and a half, the availability of the IBM FRAN program has allowed the inclusion of the effect of rigid joints in the backup structure (instead of pin-ended joints) and the development of a satisfactory grid analogy. Prior to the release of this program by IBM, the Haystack structure was used to field test the program to evaluate its usefulness as an analytical tool. The backup structure includes many rigid joints; however, the significant rigid joints are in ring 3 and the trunnion beam, where the members are quite stubby (length-to-diameter ratio ≈ 5) and are butt-welded. The effect of joint rigidity can be seen by comparing the STAIR and FRAN analytical methods. In STAIR, the resistance to displacement is only a function of the cross-sectional area of the member, while FRAN adds to this the additional stiffness resulting from the added constraint that the angular relationship of the members at each joint remain constant. This is a function of the bending and twisting inertia of the member. In addition, FRAN calculates the resulting rotations of the entire joint along with the x-y-z displacements. Thus, FRAN solves for twice as many variables at each joint as STAIR: six instead of three. These rotations are not, in general, important; however, the added displacement resistance contributed by the member bending properties is important, especially since in general it varies throughout the structure. If it were uniform throughout, it would result in reduced over-all deflections. However, it is local in nature, which can cause it to have a significant local effect on surface distortion, even though the over-all deflection change is still small. The basic parameters of FRAN, as programmed for Haystack on the IBM 7094, are indicated in Fig. 14.

One added advantage of the FRAN program is its ability to predict more adequately the behavior of a membrane shell. Early efforts using the model tests for correlation showed that good representations of the membrane and bending stiffness of the shell were not available. Additional theoretical work was done in this area with no really good results until the FRAN program became available. The shell has too many properties to be represented effectively by the single basic parameter available in STAIR, i.e., the cross-sectional area of the member. FRAN's ability to deal with bending makes it possible to develop a more exact analogy.

The FRAN program has been used in three main areas: the in-plant tests without panels, the on-site tests with the complete structure, and the operating condition of gravity loads. The degree of correlation with the various tests, as will be shown, was even better than with STAIR.

The initial FRAN run for these tests considered the structure to be completely pin-jointed, in order to make a direct comparison with the STAIR analysis. Comparison of these results showed that FRAN gave results identical to the earlier STAIR work within 0.001 inch. The data for this run were then revised to include bending rigidity of the members in ring 3 and the trunnion beams. The results of this run were then compared with STAIR and the actual tests. The difference between STAIR and FRAN are fairly small, as can be seen in Fig. 12, which is a sample of the comparisons made. The FRAN results, however, are closer than STAIR to the test results for about 70 percent of all the measured points. This is extremely good, considering that STAIR was within 0.010 inch of the test values at over 90 percent of the values, and 0.010 inch is considered to be the measurement uncertainty.

From the foregoing results, it may be concluded that, for the backup structure alone, the STAIR, FRAN, and NAA programs yield generally good results, and that computer techniques can reliably predict backup structure deflection behavior.

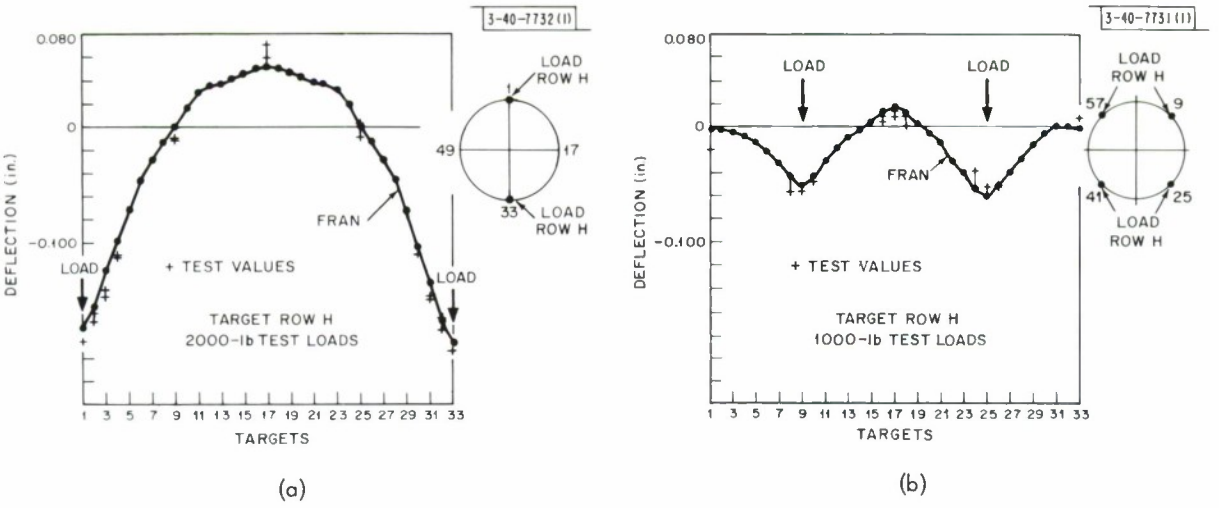

Fig. 15. Comparison between computed deflection values and on-site tests.

After disassembly, shipping, and final complete assembly at the site, more comprehensive tests were made. For these tests, the structure was complete and included its integral shell. An analytic representation of the continuous shell by means of a network of beams and bars (a lattice analogy) was developed from the theory of shells and framed structures, and checked using actual shells with known solutions available in various publications. A formulation of a shell attached to a backup structure by means of standoff studs (both the normal and shear studs) through the joints was developed and used to compute deflections. A comparison between computated deflection values based on this more complete analogy and the on-site tests can be seen in Figs. 15(a) and (b). As with the in-plant tests, the agreement between the tests and the FRAN analytical results is, in general, extremely good. Most of the analytical values are within 0.010 inch of these test values.

The amount of structural testing on the Haystack system has been much more extensive than for other comparable structures. The results have been extremely gratifying and indicate that the analytical tools (such as FRAN and STAIR) now available to structural engineers can provide data which are even more precise than can be obtained by measurement from carefully controlled full-scale tests.

This testing had one major purpose, i.e., to demonstrate the validity of the analytical model for a complete set of tests and to establish a level of confidence for the computer analysis. The test program indicated that the analysis was valid and adequate.

The gravity load cases have been run on the computer, and the results indicate general agreement with STAIR in that the peak distortions have remained at ±0.040 inch. The FRAN predicted pattern of distortion, while it is essentially the same, does show significant local difference from those obtained from STAIR. The additional effort required by the FRAN computations has proved valuable, since the surface may be adjusted in the face-up orientation to a distorted paraboloidal shape to minimize surface errors when the reflector is tilted to 45°, and errors in the bias rigging table as small as 0.020 inch could increase local distortions by up to 50 percent.

FRAN has been used to evaluate the optimum use of the three variable counterweights that have been added to the structure to permit gravity compensation of sectors of the surface. These are the two pendulum ballast beams which apply cable forces to the top of the antenna as a function

of elevation angle, while the third is the outboard counterweight system which modifies the forces on the backup structure as a function of elevation angle to give a minimum distortion to the surface.

The details of this design effort will be documented in a separate report and should prove valuable as a guide for similar structural development tasks.

III. RADOME

The desire to locate this new experimental station relatively near the M.I.T. Lincoln Laboratory dictated that the antenna must survive the rigors of a New England environment. Studies indicated that it would not be possible to construct a large, steerable microwave antenna with the required surface tolerance and pointing precision unless it were protected from the wind, snow, and ice. The use of a radome for this purpose appeared preferable to a movable shelter because it would allow the system to operate a greater percentage of time. To be acceptable, the effective noise temperature of the radome must be low, since the new experimental station would employ helium-cooled, low-noise receivers.

Prior to the start of the Haystack program, the large-diameter rigid radomes that were in use employed relatively thick dielectric walls or sandwich-type construction to fulfill the structural requirements. These thick-walled all-plastic radomes exhibited electromagnetic performance which was unacceptable at wavelengths shorter than 30 cm. Large-diameter, air-inflated radomes also suffered from similar electromagnetic limitations at wavelengths shorter than 5 cm and, in addition, did not provide the intrinsic degree of structural reliability that seemed desirable. Fortunately, studies had been started at the Lincoln Laboratory in 1957 which led to the development of a new type of radome with improved microwave performance. This new radome employed a spherical structural framework of metal beams which made it possible to use relatively thin, low-loss dielectric panels to cover most of the radome surface area. At the time that the Haystack program was being formulated, a 150-foot-diameter, metal space-frame radome, designed to withstand a 200-mph Arctic environment, was under procurement by the Air Force. This radome, which had the shape of a 5/8 sphere, was made available to Lincoln Laboratory for electromagnetic evaluation testing. Although this particular radome was designed for the Arctic and therefore over-designed for a New England environment, its use to shelter the new proposed microwave antenna was considered. Studies indicated that it would be possible to extend the lower section of the 5/8 sphere to convert it to a 9/10 sphere, and that this change could be accomplished without weakening the structure below the wind survival specification of 130 mph that had been established for the Massachusetts location.

As discussed earlier, the decision to take advantage of the availability of the 150-foot-diameter radome influenced the choice of the antenna size. An antenna diameter of 120 feet was selected because it was the largest fully steerable parabolic aperture on an elevation-azimuth mount which could be fitted into the radome. With an antenna of this size, the clearance between the radome and the rim of the reflector is about $3\frac{1}{2}$ feet. Figures 16 and 17 show the relationship of the radome to the other facilities at the site.

In the original 200-mph radome design, approximately 6 percent of the spherical surface was occupied by the metal space framework. However, since a substantial portion of the electromagnetic energy passes through the spherical radome surface at an oblique angle, the shadowing produced by the metal ribs of the radome will be greater than 6 percent. In the Haystack system,

Fig. 16. Placement of antenna within radome.

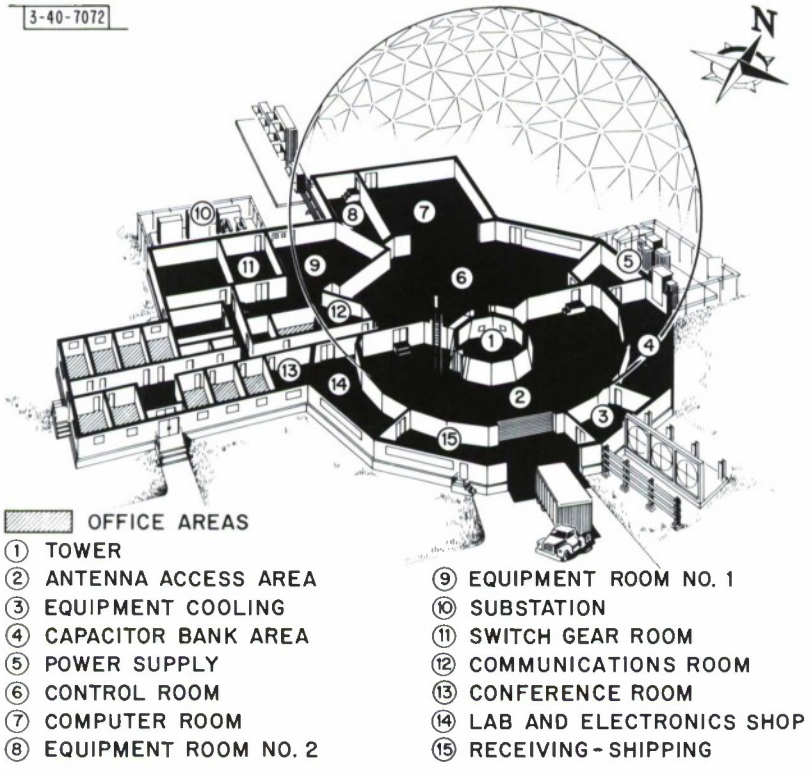

Fig. 17. Building layout.

the use of a 120-foot-diameter antenna within a 150-foot-diameter radome results in a computed effective aperture blockage of about 11 percent. Electromagnetic tests on a model range demonstrated that the noise temperature contribution of the metal space frame was small. The loss of 11 percent of the effective aperture seemed tolerable in order to obtain an improved environment for the remaining 89 percent of the antenna surface.

The metal members of the space framework vary in length between 9 and 15 feet and are aluminum extrusions approximately 3 inches × 5 inches in cross section. This framework is used to support fiberglass dielectric panels 0.032 inch thick. The loss tangent of these dielectric panels is about 0.01.

The electrical performance of this radome has been calculated and is shown in Fig. 18. Throughout the 1- to 10-Gcps frequency region, the loss attributable to the space frame is about 1.1 db. At higher frequencies, significant energy is reflected from the membrane, since it has a dielectric constant of about 4. At a frequency where the membrane thickness approaches $\lambda/2$, the reflections at the front and rear boundaries of the membrane cancel.

Only that fraction of this reflected energy which is scattered toward the ground contributes to the over-all system noise temperature. This noise contribution is a function of the antenna elevation angle, the aperture illumination, and the wavelength. Based upon calculations, a plot of this noise contribution due to backscatter from the radome for two values of aperture illumination and at two wavelengths is shown in Fig. 19.

It is clear that the performance of this radome, while perhaps acceptable, is not ideal. Today, it is possible to design a more satisfactory space-frame radome in the 150- to 200-foot-diameter class with an over-all loss of perhaps only 0.5 db. This could be accomplished by designing the structural members for a 130-mph environment, instead of the 200 mph as employed for this particular design, and by constructing the beams from high-tensile-strength steel instead of aluminum. By employing presently available digital computer analytic techniques, a more efficient space-frame design also seems feasible. The use of a radome that is larger in proportion to the antenna diameter would also reduce the electrical shadowing. Radome membrane

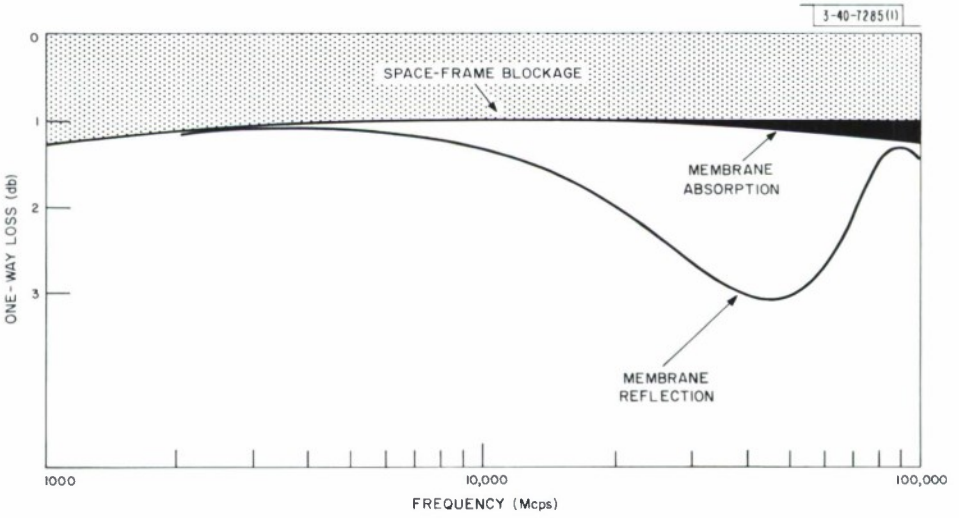

Fig. 18. Electrical performance of rodome.

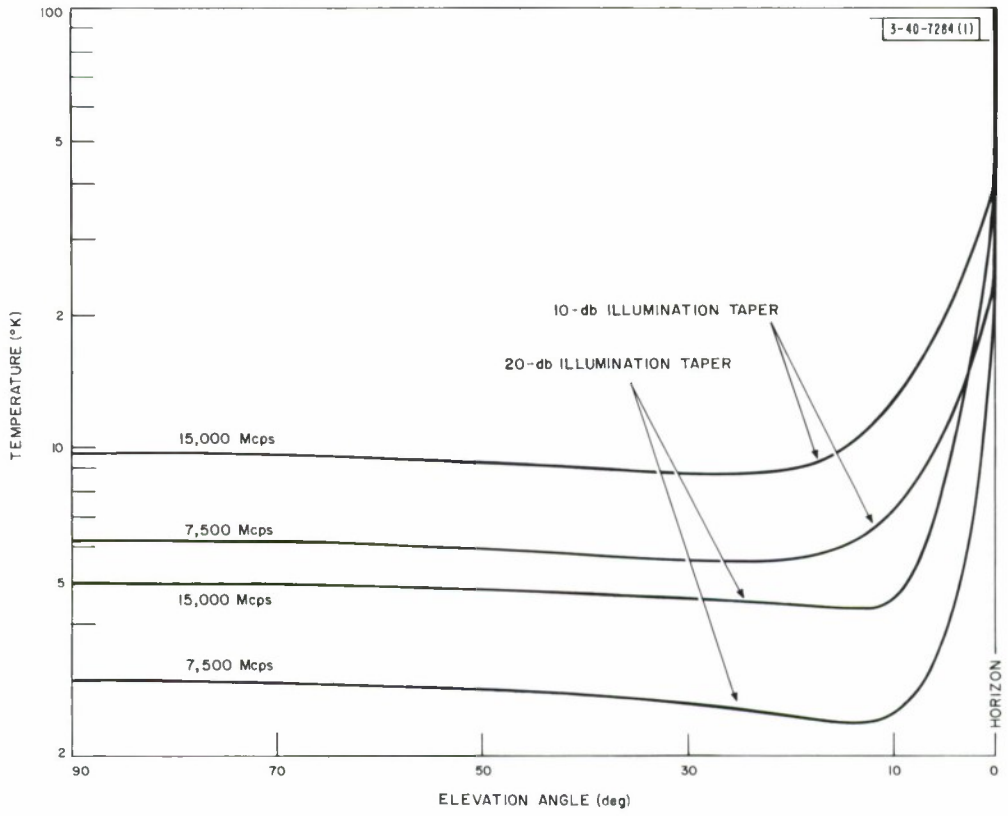

Fig. 19. Rodome noise contribution.

materials with improved characteristics are now available, and these new materials will make it feasible to use thinner membranes which will improve the electromagnetic performance of the radome at the higher frequencies.

IV. PLUG-IN ELECTRONICS EQUIPMENT

To facilitate the use of the Haystack system over a wide frequency range and for a variety of experiments, the antenna structure has been designed to accommodate plug-in equipment rooms. These equipment rooms will be used to house low-noise receiver components, cryogenic equipment, and the final amplifier of high-power microwave transmitters. Provision has been made to mount any one of a number of interchangeable equipment rooms directly behind and along the axis of the main parabolic reflector. This equipment configuration is efficient, since it makes it feasible to mount the primary antenna feed horn directly onto the face of the plug-in room and eliminates the need for rotary joints and long runs of waveguide. An integral hoist system has been provided to raise and lower an 8-foot × 8-foot × 12-foot plug-in room with a maximum weight of 7000 pounds. A typical plug-in equipment room is shown in Fig. 20.

Since it is not intended that operating personnel will remain within the plug-in room when the antenna is in use, provision has been made to control and monitor the electronic equipment remotely. Since the equipment room rotates ±300° in azimuth and 90° in elevation, cable-wrap systems have been incorporated into the antenna structure. Special cables were procured to obtain the desired compliance and to insure that they would survive repeated flexing.

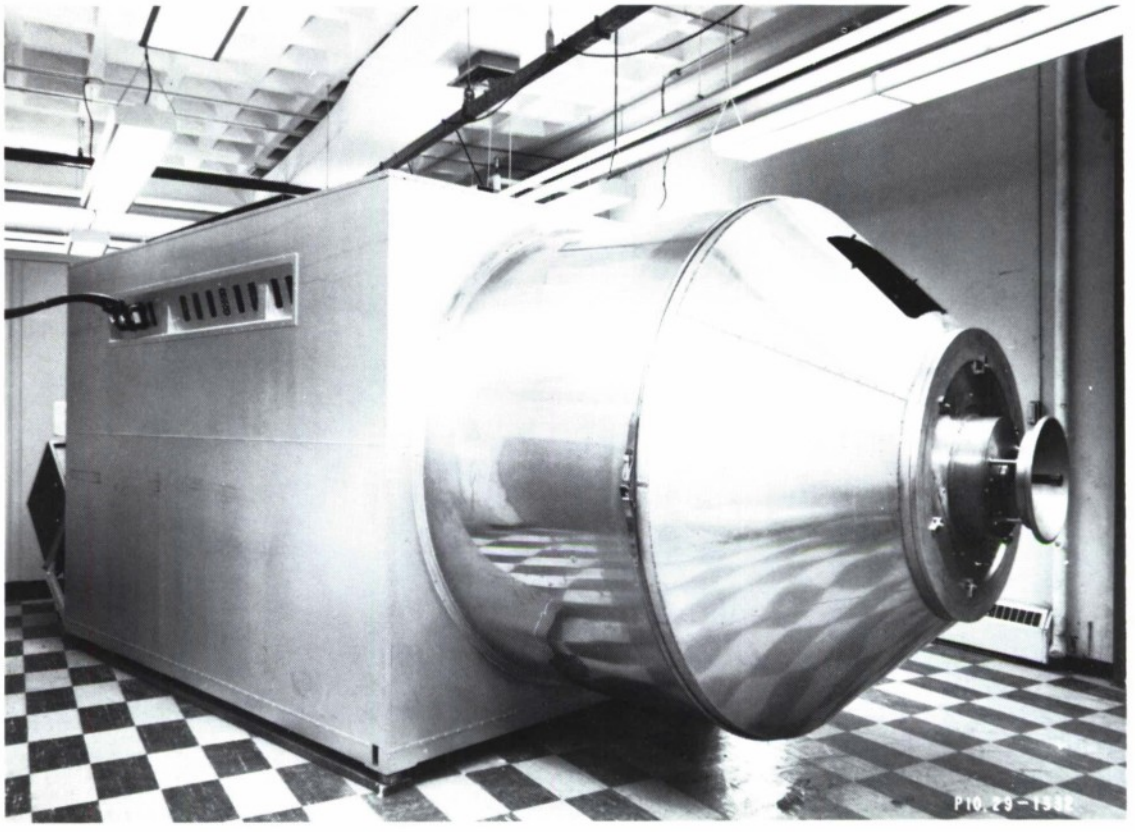

Fig. 20. Typical plug-in equipment room.

Provision has also been made to operate the plug-in equipment room at either of two test stands on the ground. A versatile interconnection system has been provided to permit the simultaneous operation of one plug-in room in the antenna while a second plug-in room is under test at the ground stand. High-quality, multiconductor plugs and jacks are employed to allow rapid patching of the approximately 3000 power and control leads and the several hundred coaxial connections that are provided. For transmitter operations, high voltage, compressed air, and up to 260 gallons of cooling water per minute are also available at the plug-in box locations in the antenna and on the test stands. Figure 21 is a photograph of the plug-in patch panel in the main control room. All the connecting plugs are keyed and interlocked.

One of the test stands is situated outside the radome, approximately 150 feet from the main antenna location, to permit radiometric measurement unimpeded by the radome. A photograph of the plug-in equipment room in this test stand is shown in Fig. 22.

V. ANTENNA CONTROL SYSTEM

To utilize a high-gain steerable antenna effectively, it is necessary to be able to point the antenna beam with an uncertainty not greater than 1/10 of a beamwidth. In addition, there are experiments which could utilize a beam-pointing capability as precise as 1/100 of a beamwidth. With the Haystack antenna, where the half-power beamwidth will be 0.05° at a wavelength of 3 cm, the fulfillment of even the 1/10 beamwidth requirement under dynamic conditions requires a sophisticated control system.

Fig. 21. Interconnection patch panel.

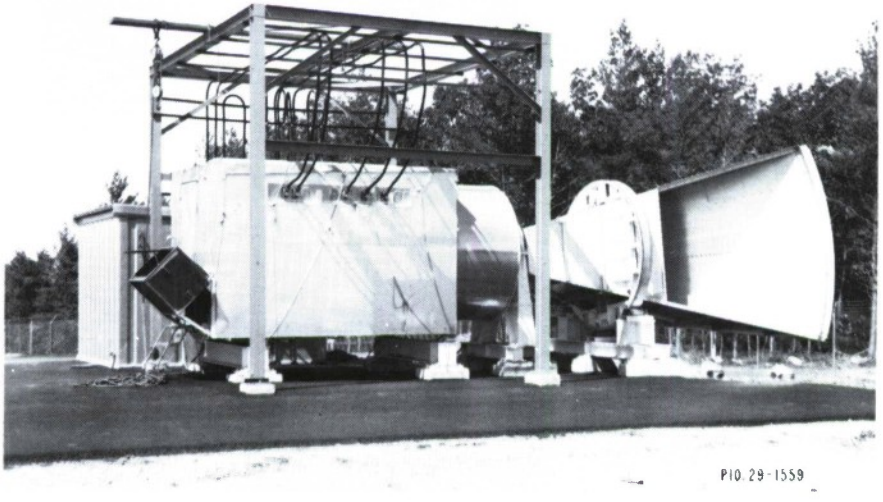

Fig. 22. Radiometer test stand.

The pointing problem is most severe for low-altitude satellite targets because they pass through the narrow antenna beam at high angular rates. For example, a 200-mile-high satellite at closest approach will have an angular rate of approximately 1° per second as seen from a ground station, whereas a satellite at a 2000-mile altitude at closest approach will move through the beam at an angular rate of 0.1° per second. Targets such as the moon, the sun, planets, and stars have angular rates of approximately 0.004° per second, determined largely by the earth's rotation. Hence, even distant targets of interest, such as radio stars, will pass in and out of the beam in a period of less than 15 seconds. Since the antenna will permit angular rates as high as 3° per second, the pointing system must achieve smooth motion with high precision.

In the Haystack system, a high-speed, general-purpose digital computer is used in the (real-time) control system. In addition to the computer pointing control, backup facilities in the form of manual digital controls and cruder manual analog controls also have been provided. A very simplified pointing system diagram is shown in Fig. 23. The computer is intimately connected to the antenna environment; these connections are shown in Fig. 24.

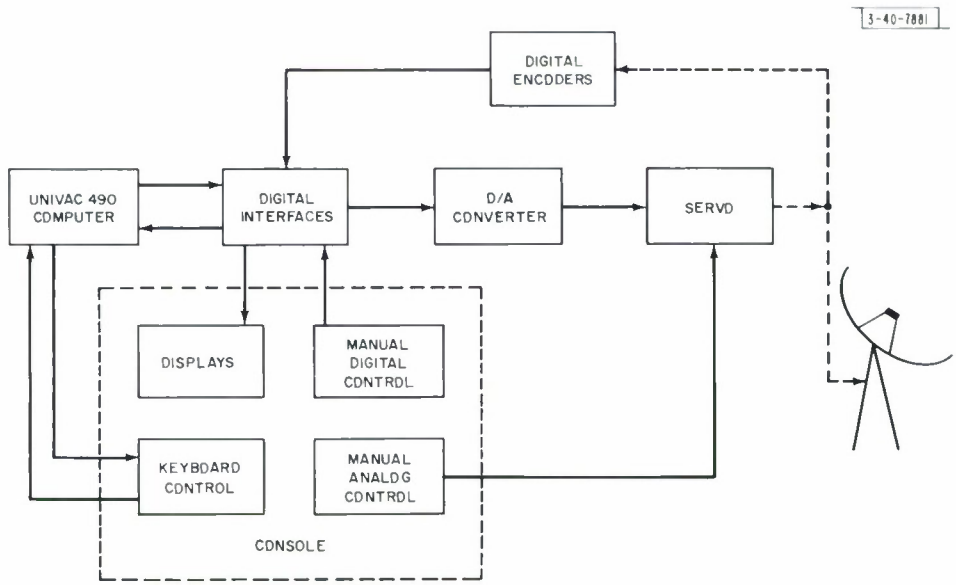

Fig. 23. Antenna control system.

The computer permits a relatively unskilled operator to control and direct the antenna in a precise manner. Through the use of a standard typewriter keyboard, the operator can request the antenna to point to designated coordinates or follow one of many preplanned tracking sequences. Software programs have been prepared which permit an operator to request that the antenna point at such targets as the moon, the planets, and known satellites by simply typing the name of the object in clear text. The computer responds in clear text via the teleprinter and, if necessary, will ask the operator for additional pertinent information. The operator may easily interject modifications to the routine in use and can easily employ one of a number of scan and search modes. The program system itself is shown diagrammatically in Fig. 25. The program functions shown on the left portion of this figure are interspersed with the main position command loop on a time-shared basis.

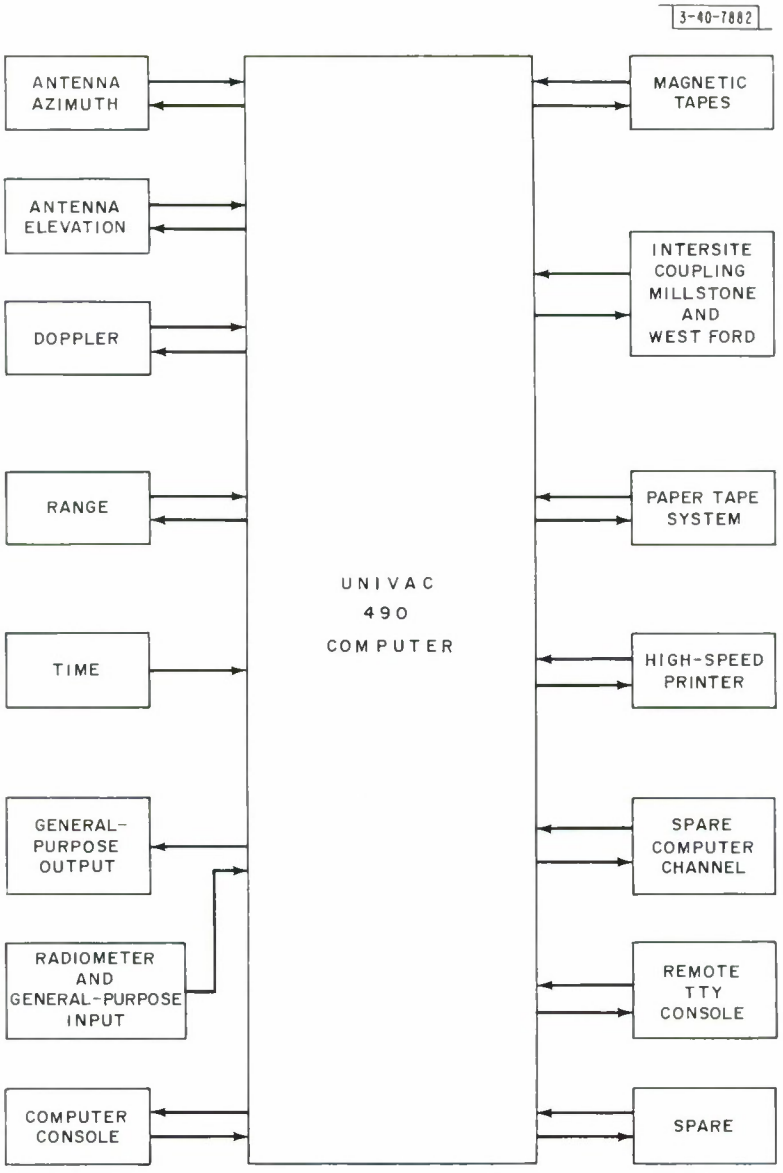

Fig. 24. Connections to Univoc 490 computer.

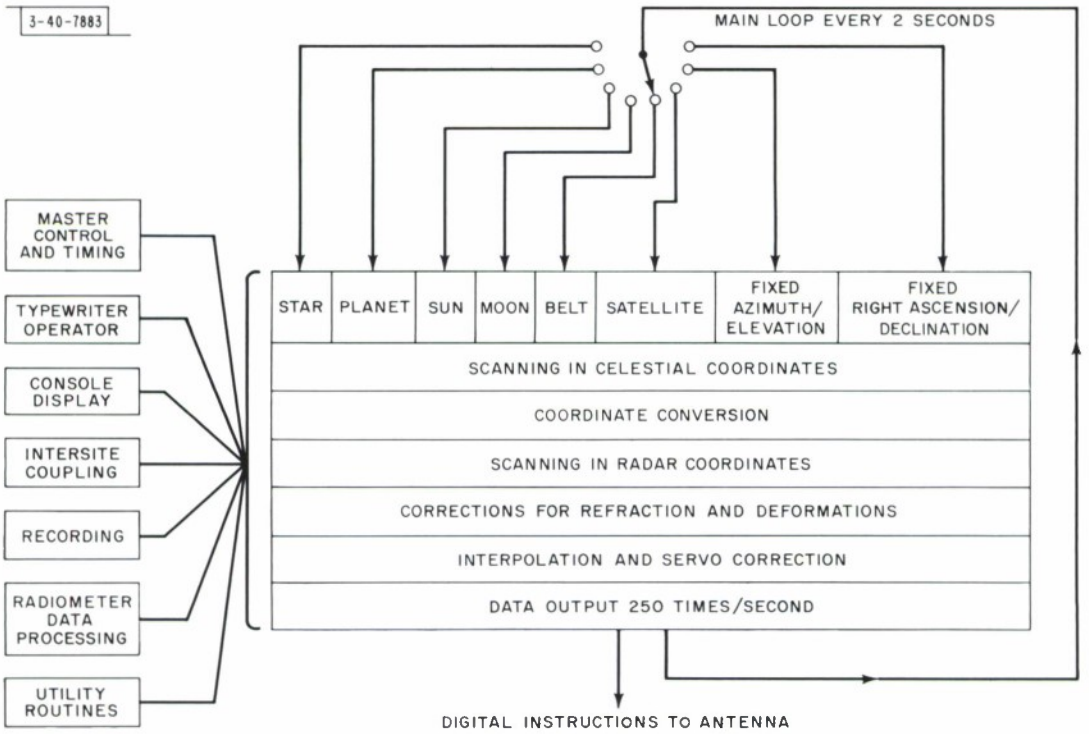

Fig. 25. Computer program organization.

Fig. 26. Univac 490 computer in control room.

The computer has been programmed to permit the pointing system to compensate for systematic errors in the antenna structure and data-take-off components. At low elevation angles, where the refractive index of the atmosphere will influence the beam pointing position, the computer will be used to introduce corrections to compensate for this effect, and these pointing corrections can readily be modified whenever appropriate. Once an object type has been selected by an operator, a main computer program cycle takes place every 2 seconds. At that time, the new position of the object is determined, superposition of selected scanning takes place, and the position is transformed from celestial to radar coordinates. Corrections for refractive and structural deformation are superposed, and 4-point interpolation is used to determine the 250 points per second required to provide smooth direction of the antenna servo system.

The computations to find positions of stars, planets, the sun, and the moon are found by preliminary interpolation in stored magnetic tape tabulation of basic Nautical Almanac data. Positions of earth satellites and the West Ford belt are found by direct evaluation of the satellite equations from a starting point of orbit parameters.

Extra effort has been expended to permit easy use of the facility. As an example, the system can be run in speeded-up time to serve as a planning device; thus, one can easily determine the precise conditions to be expected in azimuth, elevation, range, and Doppler for a particular planetary observation some time in the future. Even while a tracking sequence is in operation, the operator may interact with the computer system to modify the pointing control mode. The computer also makes it possible for the Haystack system to accept pointing information from remote sources and to make this information useful for directing the Haystack antenna. This involves the generation of parallax and time-delay corrections in real time. The computer also provides a capability for preparing pointing information to be sent from Haystack to other locations in a form compatible with external sensors.

Computer programs have also been prepared to calibrate the servo-response function of the antenna. A number of interesting new diagnostic techniques are expected to evolve from this flexible capability.

A photograph of the Sperry Rand Univac 490 digital computer, as installed at the Haystack facility, is shown in Fig. 26. This computer was chosen because its word length of 30 binary bits and its input-output system were compatible with the pointing precision requirements and because its computational speeds permitted the generation of pointing commands in real time from orbit parameters. One of the unique features of this computer is its flexible input-output system which permits the computer to time-share functions. With this capability, several input and output devices can supply and receive data without interfering with other computer functions.

VI. FREQUENCY CONTROL AND TRANSLATION EQUIPMENT

The frequency translation system is designed to produce precise frequencies for use in exciting various transmitters and for appropriate coherent reference signals for use in the detection and data-processing channels.

The basic frequency standards at the station are the Varian model V-4700 rubidium vapor frequency standard and the Hewlett-Packard 107 crystal oscillator. These units are checked against the U.S. national frequency standard by comparison methods, using HF and VLF broadcast time and frequency signals. The long-term accuracy of the frequency standard system as determined by the rubidium unit is 5 parts in 10^{11} per year. The short-term performance of

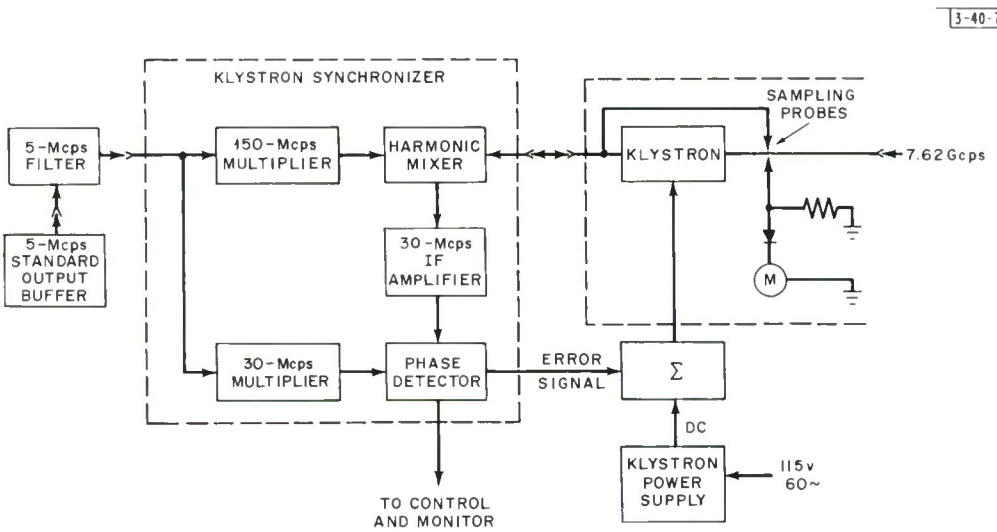

Fig. 27. Local ascillatar stabilizing system.

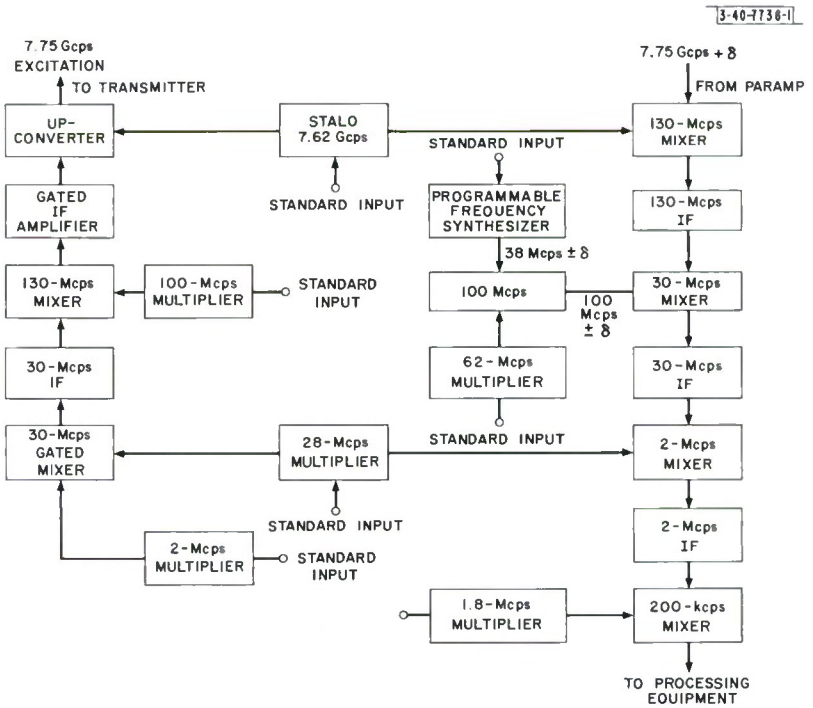

Fig. 28. Frequency translatian system.

this equipment is 1 part in 10^{11} for a one-second average time. The crystal oscillators are checked against the rubidium standard and serve as flywheels, which can continue in operation in the event of power failure.

Various frequencies are derived as multiples or subharmonics of the standard reference frequencies of 1 and 5 Mcps. These frequencies are used to drive synthesizers and synchronizers which produce frequencies in 10-Mcps increments up to a limit of about 12 Gcps. For example, the configuration used to provide the stabilized local oscillator for a 7.75-Gcps radar is shown in Fig. 27. Multiplier chains are used to develop 30- and 50-Mcps harmonics for use as reference standards in the klystron synchronizing system. A 1-watt X-band source having essentially monochromatic spectral characteristics with the same intrinsic stability as the crystal oscillator is produced.

Frequency translation equipment (Fig. 28) is used to produce the desired transmitter frequency and the IF frequencies required for processing the received signals. The first IF frequency is 130 Mcps. For transmitting, it is synthesized by heterodyning the appropriate harmonics of the standards. Special modulating signals and pulsing can be applied to any of the higher-frequency signals. A varactor diode up-converter is used to combine the 130-Mcps IF with the 7.62-Gcps stabilized local oscillator to obtain the RF excitation for the transmitter. The stalo, of course, serves as the first local oscillator in the receiver chain and heterodynes the received signal down to the 130-Mcps first-IF frequency. A second heterodyne conversion produces an IF of 30 Mcps.

The first-IF amplifier chain, operating with a cooled parametric amplifier in front of it, has a measured dynamic range of 87 db in a 1-kcps noise band.

A 100-Mcps local oscillator is developed by adding the output of a programmable frequency synthesizer to the 62-Mcps harmonic of the frequency standard. The Doppler shift of the received signal can be removed by using a precomputed ephemeris table with an accuracy of 1 cps and a precision of 0.1 cps. Subsequent heterodyne translations are used successively to provide receiver channels with 2-Mcps, 200-kcps, and 5-kcps intermediate frequencies, depending on the application. Planetary and lunar radar experiments will use the narrow-bandwidth 5-kcps intermediate frequency. If the signal-to-noise ratio is adequate, a detector system in the 5-kcps IF channel can be used to develop a phase-locked reference for closed-loop Doppler tracking.

VII. THE RADIOMETRIC SYSTEM

The Haystack radiometric system has been designed for research investigations of our own atmosphere, the moon, the planets, stellar radio sources, interstellar gas clouds, and external galaxies. Radiometers operating at frequencies of 5, 8, and 15.5 Gcps have been completed and, by July 1965, radiometers will be added for 1.42 Gcps (hydrogen-line frequency), 1.67 Gcps (OH-line frequency), and 35 Gcps.

The radiometric system employs several concepts and devices which are new to radio astronomy. A novel approach has been taken in the following areas:

(a) Wide-band tunnel-diode amplifiers have been used for the input amplifier in the 5-, 8-, and 15.5-Gcps radiometers. Since radiometer sensitivity is proportional to the system noise temperature divided by the square root of the RF bandwidth, a tunnel-diode receiver with 1000° system

temperature and 1000-Mcps bandwidth is equivalent to a maser or paramp receiver with 100° system temperature and 10-Mcps bandwidth. The reliability, stability, and absence of cryogenic equipment makes the use of tunnel diodes very attractive.

(b) As discussed in Sec. IV, the plug-in antenna room makes it relatively easy to maintain and change radiometer equipment.

(c) A precision square-law detector, synchronous detector, and integrator have been designed for use with high-accuracy digital processing. The synchronous detector and integrators are solid state and have a drift which is 0.01 percent of maximum output.

(d) A flexible data system has been utilized which can couple any combination of seven 30-bit digital data sources and sixteen analog data sources to a computer, a paper-tape punch, or a printer at a fast, buffered rate. In addition, fifty sets of analog data, representing monitor points in the system, can be fed into any of the above devices at a slow unbuffered rate.

(e) Real-time processing of radiometric data will be accomplished in the digital computer that is also employed for antenna pointing. A program is completed which calibrates the radiometer output and prints and plots antenna temperatures. The computer also checks the fifty radiometer monitor points to see if they fall within limits. Extensive use of the on-line computer for radiometer control, monitoring, and data analysis is anticipated.

(f) The spectral-line receivers will utilize an accurate and versatile digital autocorrelator for spectral analysis. A 100-channel, 10-Mcps clock-rate correlator is under construction.

A photograph of the radiometer equipment room is shown in Fig. 20. The circular extension on the front of the room supports the antenna feed. Future cryogenic front-end equipment will be mounted in this circular extension, in close proximity to the antenna feed.

Normally, the complete RF portion of a radiometer will be installed in the equipment room, and the synchronous detectors, integrators, and data-processing equipment will be located in the control room. However, a complete radiometer system with analog pen-recorder output can be operated from the equipment room for testing purposes.

The temperature environment of radiometric front ends is extremely critical. For example, if a front-end component has a small loss of 0.25 db and its temperature changes by 2°C, a 0.1°K spurious signal will be introduced into the radiometer. Since the inherent sensitivity of the radiometers in use is of the order of 0.01°K for $\frac{1}{2}$ hour of integration, this is a serious error. A high degree of temperature stability has been achieved in the radiometer room by using proportionally controlled heaters in conjunction with an air conditioner. The heater-control loop senses the temperature of the air entering the room and holds this to within ±0.1°C for one-hour periods and ±0.25°C for 24-hour periods. The room is well insulated and good radiometer stability has been obtained.

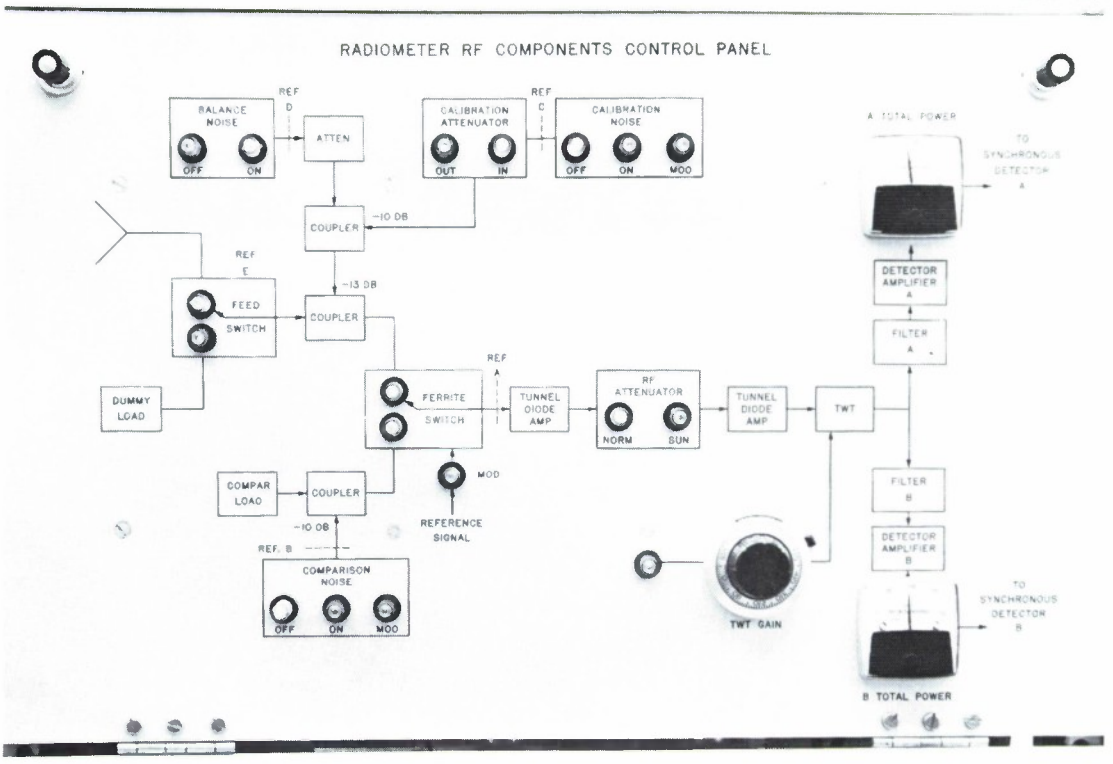

Fig. 29. Radiometer control panel.

A typical radiometer RF components control panel is shown in Fig. 29. In normal operation the feed switch is in the antenna position, the comparison noise source and calibration noise source are off, the balance noise source is on, the ferrite switch is modulated at a 40-cps rate, and the RF attenuator is in the normal (no attenuation) position. The ferrite switch is then switching the receiver input between the comparison load (a thermally insulated termination at 300°K) and the antenna with balance noise (~ 300°K) added. A 40-cps signal whose amplitude is proportional to antenna temperature is thus produced at the detector output, where it is amplified, synchronously detected, and integrated.

The basic receiver is of the TRF type. A 4-stage tunnel-diode amplifier followed by a single traveling-wave tube amplifier is used. The TWT stage is needed because the maximum linear output of present tunnel-diode amplifiers is not quite enough to properly drive the diode detectors. The characteristics of the amplifier chain are: 60-db gain, 1000-Mcps bandwidth, and system noise temperatures of 1000°K at 5 and 8 Gcps and 2500°K at 15 Gcps. The output of the amplifier chain is divided into two 500-Mcps bandwidth bands (for interference detection purposes) before detection.

The link between the radiometers and the data-recording system is through a synchronous detector-integrator designed for operation on radiometer signals which are to be digitally processed. Most commercial synchronous detectors are designed for analog recording or display purpose and have drift and noise which is of the order of 0.5 percent of maximum output. The design goal of this unit is drift and noise levels which are 0.01 percent of maximum output because the post-integration signal-to-noise ratio on strong sources will approach 10,000 to 1 and

the A/D conversion equipment has an accuracy of 0.01 percent. In addition, the wide-dynamic-range synchronous detector makes scale changes unnecessary and simplifies observations.

The synchronous detector contains both an RC integrator for analog pen-recorder display and a true finite-time integrator for digital recording equipment. The true integrator is sampled by a high-speed A/D converter at the conclusion of the integration period, which can be varied between 0.3 second and 30 seconds. The high-speed A/D converter can be used to sample many true integrators. This is a more flexible and economical approach than the method commonly used in radio astronomy of using an integrating type of A/D converter for each radiometer channel. The synchronous detector contains a post-detection gain modulator, which is an innovation to radiometry. The synchronous detector is all solid state, utilizing approximately 75 transistors.

Radiometer data are collected in two types of scans: a data scan for the main radiometer data and an auxiliary scan for monitoring data. In the data scan, 16 sources of analog data are multiplexed into an A/D converter and the analog voltages are converted into 17-bit digital numbers. In addition, 7 sources of digital information are scanned. These 23 words of data are collected in 23 milliseconds and are stored in a circulating delay-line memory. Any combination of these 23 data words can then be fed into either a printer, a paper-tape punch, or the Univac 490 computer. A new data scan is initiated periodically at adjustable intervals between 0.1 second and 100 seconds. The auxiliary scan consists of a stepping switch which will scan up to 50 sources of analog monitor data. This information is converted in the same 17-bit A/D converter as the analog data scan data and can be fed into either a printer, a paper-tape punch, or the computer.

-40-7756

RELATIVE TEMPERATURE (°K)

TIME	RIGHTA	DECLIN	T(1)	T(2)	DEL(1)	DEL(2)	-0.5 0.0 0.5 1.0
06 34 47	23 24 59	58 36 27	-0000.05	-0000.06	00.02	00.02	I 1
06 35 15	23 25 25	58 36 27	-0000.06	-0000.00	00.02	00.02	I XO
06 35 45	23 25 55	58 36 27	0000.03	-0000.05	00.02	00.02	I O X
06 36 15	23 26 25	58 36 27	-0000.05	-0000.01	00.02	00.01	I XO
06 36 45	23 26 55	58 36 27	-0000.03	-0000.04	00.02	00.01	I 1
06 37 15	23 27 26	58 36 27	-0000.03	-0000.00	00.02	00.03	I 1
06 37 45	23 27 56	58 36 27	0000.01	0000.01	00.01	00.02	I 1
06 38 15	23 28 26	58 36 27	-0000.05	0000.02	00.02	00.02	I X 0
06 38 45	23 28 56	58 36 27	0000.00	0000.02	00.02	00.02	I 1
06 39 15	23 29 26	58 36 27	0000.03	0000.01	00.02	00.02	I 1
06 39 45	23 29 56	58 36 27	0000.01	-0000.06	00.01	00.02	I O X
06 40 15	23 30 26	58 36 27	-0000.04	0000.00	00.01	00.02	I XO
06 40 45	23 30 56	58 36 27	0000.03	0000.03	00.01	00.03	I 1
06 41 15	23 31 26	58 36 27	0000.08	0000.05	00.03	00.03	I 1
06 41 45	23 31 56	58 36 27	0000.08	0000.11	00.02	00.02	I XO
06 42 15	23 32 26	58 36 27	0000.14	0000.09	00.03	00.03	I OX
06 42 45	23 32 56	58 36 27	0000.08	0000.05	00.02	00.02	I 1
06 43 15	23 33 26	58 36 27	0000.17	0000.13	00.02	00.03	I OX
06 43 45	23 33 57	58 36 27	0000.29	0000.17	00.02	00.03	I O X
06 44 15	23 34 27	58 36 27	0000.26	0000.28	00.02	00.03	I 1
06 44 45	23 34 57	58 36 27	0000.31	0000.31	00.03	00.03	I 1
06 45 15	23 35 27	58 36 27	0000.38	0000.39	00.02	00.02	I 1
06 45 45	23 35 57	58 36 27	0000.49	0000.45	00.03	00.03	I 1
06 46 15	23 36 27	58 36 27	0000.54	0000.56	00.03	00.03	I XO
06 46 45	23 36 57	58 36 27	0000.59	0000.55	00.02	00.03	I 1
06 47 15	23 37 27	58 36 27	0000.64	0000.62	00.02	00.02	I 1
06 47 45	23 37 57	58 36 27	0000.71	0000.71	00.02	00.02	I 1
06 48 15	23 38 27	58 36 27	0000.76	0000.74	00.02	00.03	I OX
06 48 45	23 38 57	58 36 27	0000.84	0000.81	00.02	00.02	I 1
06 49 15	23 39 27	58 36 27	0000.78	0000.78	00.03	00.02	I 1
06 49 45	23 39 58	58 36 27	0000.82	0000.78	00.03	00.02	I OX
06 50 15	23 40 28	58 36 27	0000.80	0000.79	00.02	00.02	I OX
06 50 45	23 40 58	58 36 27	0000.75	0000.75	00.03	00.02	I 1
06 51 15	23 41 28	58 36 27	0000.75	0000.70	00.02	00.02	I OX
06 51 45	23 41 58	58 36 27	0000.66	0000.64	00.03	00.03	I OX
06 52 15	23 42 28	58 36 27	0000.60	0000.56	00.02	00.02	I OX
06 52 45	23 42 58	58 36 27	0000.48	0000.43	00.02	00.03	I OX
06 53 15	23 43 28	58 36 27	0000.44	0000.41	00.02	00.03	I 1
06 53 45	23 43 58	58 36 27	0000.41	0000.34	00.02	00.02	I O X
06 54 15	23 44 28	58 36 27	0000.33	0000.26	00.03	00.01	I OX
06 54 45	23 44 58	58 36 27	0000.33	0000.21	00.02	00.01	I O X
06 55 15	23 45 28	58 36 27	0000.24	0000.13	00.01	00.02	I O X
06 55 45	23 45 59	58 36 27	0000.17	0000.13	00.02	00.02	I OX
06 56 15	23 46 29	58 36 27	0000.13	0000.02	00.02	00.03	I O X

Fig. 30. Sample of high-speed printer output.

An initial radiometer data-processing program has been written which provides calibrated values of antenna temperatures in real time. A sample of a high-speed printer output from this program is shown in Fig. 30. From left to right the columns of printer output represent time, right ascension, declination, antenna temperatures in data channels 1 and 2, and rms fluctuations of these antenna temperatures. The right-hand side of the printer page is devoted to a plot of antenna temperatures.

VIII. THE TRANSMITTER POWER SUPPLY AND HEAT EXCHANGER

The Haystack plug-in equipment room concept has made it feasible to operate over a wide frequency spectrum in both radar and communication modes. For this reason, it was deemed important to provide a power supply and cooling system that could operate with a variety of transmitter tubes, including klystrons, traveling-wave tubes, and amplitrons, in CW and pulsed applications. In an attempt to obtain reasonable balance between the cost of the transmitter and the other relatively expensive components necessary in the experimental system, it appeared appropriate to install a versatile high-voltage power supply with approximately a 1-megawatt DC output capability. This capability was greater than needed to supply the microwave transmitter power tubes that were available in 1960, but seemed approximately correct for the improved transmitter tubes anticipated during the next decade. For this reason, a power supply and cooling system have been specified which are somewhat larger and more versatile than those commonly found in typical radar and communication systems.

The specifications of the power supply may be summarized as follows:

Average Power:— The high-voltage DC supply shall be capable of producing, on a continuous basis, 1000 kw of DC power at any voltage from 20 kv to 120 kv.

Ripple:— The maximum peak-to-peak ripple of the power-supply DC output voltage shall be one-half of one percent of the output voltage under any combination of voltage and power output.

Energy Storage:— Sufficient energy storage shall be included to limit the voltage droop to 4 percent of the initial voltage when the supply is delivering a 2-msec pulse containing 10,000 joules of energy.

Pulsewidths:— The supply shall be capable of delivering energy to a modulator in the form of pulses of up to 10,000 joules at pulsewidths of 2 msec and greater.

Pulse Repetition Rates:— The supply shall be capable of delivering its energy to a modulator at any pulse repetition rate at which the average rating of the supply is not exceeded.

Voltage Changes:— The output voltage shall be capable of continuous adjustment from zero to any voltage in the specified operating range. Power-supply components may be connected in various configurations to allow the attainment of the full output power within each of several voltage ranges.

Polarity:— The power supply shall be capable of operating with either the negative or positive output terminal grounded.

The power supply was procured by the Air Force from Energy Systems, Inc., Palo Alto, California (formerly Radiation at Stanford). In the ESI design, the required flexibility is achieved by the use of a plate transformer which has three primary windings and six independent secondary windings. Four of the different transformer connection configurations which are available

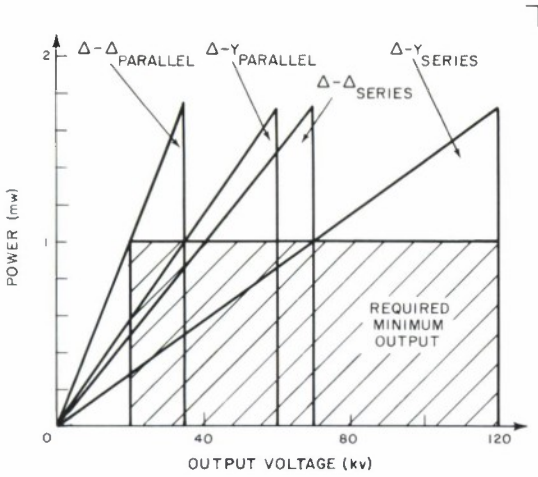

Fig. 31. Capability af pawer supply as a functian af valtage.

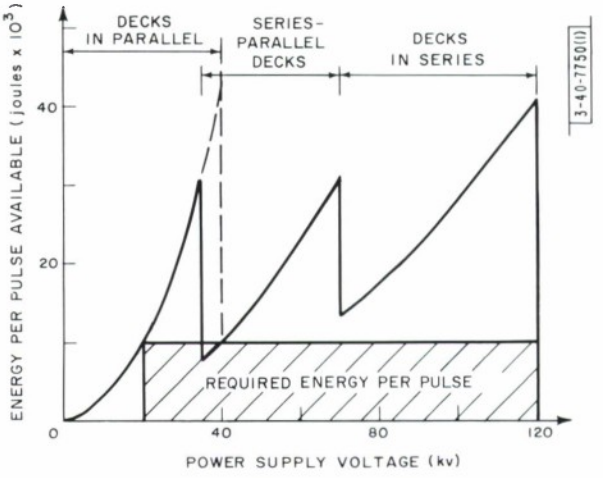

Fig. 32. Energy per pulse available for 4-percent valtage draap.

Fig. 33. Capacity energy storage bank.

will be used. There are $\Delta - \Delta$ and $\Delta - y$, with the secondary windings connected in parallel for low-voltage, high-current operation and in series for high-voltage, low-current operation. The four ranges of voltages thus available are 0-35 kv, 0-60 kv, 0-70 kv, and 0-120 kv. Since the supply must be capable of delivering 1000 kw at 20 kv, there is actually more than 1000 kw available at various other voltage levels, as indicated in Fig. 31.

The rectifiers used in this supply are semiconductor diode stacks. The diodes were chosen because they could supply the required load current with large overcurrent capability. This overcurrent capability is an important consideration for the prevention of damage to a rectifier string in the event of power-supply faults or external circuit failures. The peak current in a rectifier stack is limited by the reactance of the transformer windings. The reactance has been chosen both to limit the current and to serve as part of a filter, to meet the ripple requirements without the use of a separate choke. The use of semiconductor rectifiers eliminates the need for high-reactance, heater-isolation transformers which would be required if thermionic diodes were used. In addition, the interconnection of the rectifiers for operation at the various voltage levels and power-supply polarity is simplified.

The 4160-volt, 3-phase, 60-cycle input to the power supply goes through the usual fused disconnect switch and high-speed vacuum switches, which should respond in less than one cycle. An Inductrol is used to control the input to the plate transformer, allowing essentially continuous voltage variation. A DC feedback regulator loop on the Inductrol serves to regulate the voltage output of the supply to within ± 1 percent over a 25- to 100-percent output range.

The energy storage bank is composed of three decks, each consisting of 124 capacitors rated at 1.68 μf each at 40 kv. These decks may be connected in parallel, series-parallel, or series configuration. By so doing, one may obtain 625 μf at 40 kv with all decks in parallel, 70 μf at 120 kv with all decks in series, and 156 μf with a series-parallel combination of decks. The energy storage per pulse available within the constraint of 4-percent voltage droop at the various voltage ranges of the power supply is depicted in Fig. 32. The capacitor bank is designed with mechanical shorting bars which discharge the capacitors whenever the system is de-energized. The individual capacitors have series current-limiting resistors to prevent catastrophic discharging of a deck of the bank into a faulty capacitor on that deck, and also to limit the peak current which can be drawn under fault conditions. Figure 33 shows the capacitor bank.

A test load is provided so that power-supply operation can be verified over its entire range. The load consists of several water columns in parallel. The resistivity of the column is controlled by varying the salinity of the solution flowing in the columns. A heat exchanger associated with the dummy load transfers the heat generated in the dummy load into the main system heat exchanger.

The system heat exchanger is a double closed-loop system. A distilled-water loop is provided for cooling the transmitter tubes and components. An intermediate liquid-to-liquid exchanger transfers the heat from the closed-loop distilled-water system to an ethylene-glycol system which includes a liquid-to-air heat exchanger. The heat exchange problem in this system is not a simple one, since the major heat source, the transmitter, is located on the antenna a considerable distance away from the intercooler. A highly effective temperature control system is needed to minimize phase fluctuations of the transmitted signal due to variations in the body-cooling water temperature.

In a system with 500,000 joules of stored energy, a fast-acting protective circuit is essential to remove the DC from the transmitter in the event of an arc. A crowbar circuit is used which

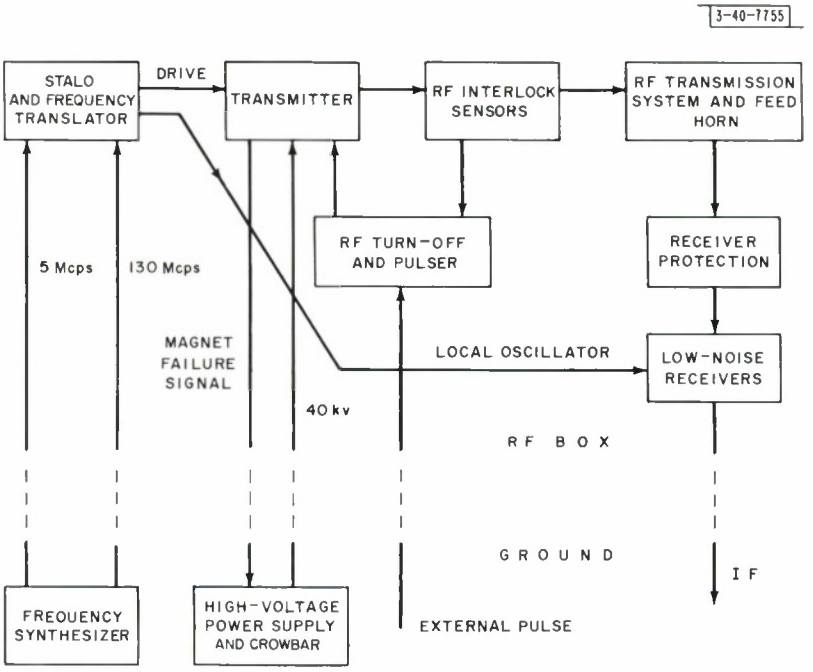

Fig. 34. Simplified diagram af transmit-receive system.

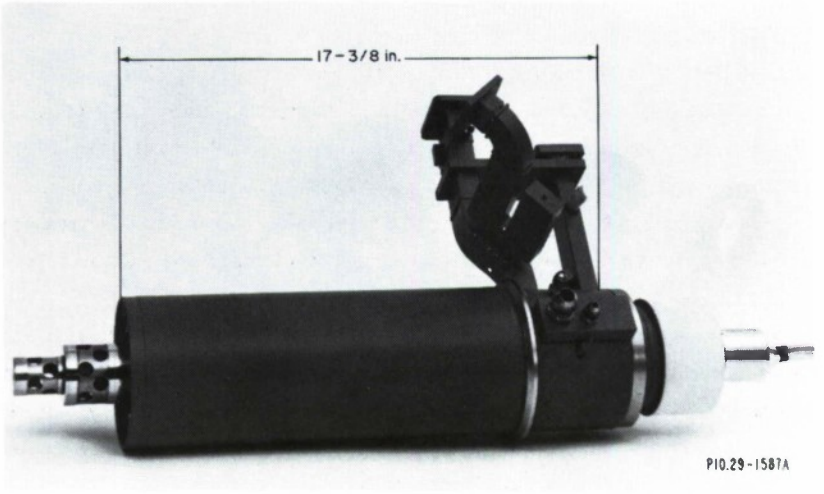

Fig. 35. VA-879 100-kw klystron.

is proprietary to Energy Systems, Inc. It is a two-ball gap which has a triggering "needle" located on the equipotential plane between the two gaps. The input-logic circuits are designed to operate in the event of excess tube current (an arc), capacitor failure, or capacitor bank overvoltage. One of the important features of the crowbar triggering system is that it provides a number of sequential triggers closely spaced in time. This prevents damage to the system which could result were the crowbar arc to extinguish before the primary power circuits opened.

IX. THE INITIAL HIGH-POWER COMMUNICATIONS-RADAR SYSTEM

The initial high-power X-band plug-in equipment room has been designed for Venus radar experiments and for communications experiments requiring simultaneous transmission and reception. This plug-in room contains:

(a) The microwave portions of the frequency synthesizer,
(b) A 100-kw, 7750-Mcps transmitter,
(c) High-power microwave circuits and feed system,
(d) Low-noise receivers.

A simplified block diagram is shown in Fig. 34.

The microwave portion of the frequency synthesizer consists of a frequency multiplier, a phase-locked klystron, and a single-sideband modulator. The frequency synthesizer derives the required frequencies from a 5-Mcps crystal oscillator with appropriate multiplication. The phase-locked klystron provides the required local oscillator power at 7620 Mcps and also furnishes RF power to the single-sideband modulator, whose output is the transmitter drive signal and is offset from the local oscillator by the 130-Mcps intermediate frequency.

A VA-617 traveling-wave tube is used to drive a VA-879 5-cavity klystron final amplifier (Fig. 35). This klystron, recently developed by Varian Associates, Palo Alto, California, has an output power of 100 kw CW, a gain greater than 50 db, a 3-db bandwidth of about 40 Mcps, and an over-all efficiency greater than 40 percent.

Figure 36 shows the principal features of the RF amplifier chain. Of special interest are the protective circuits which have been incorporated to prevent damage to the tube if an arc should occur in the waveguide system. Two types of protection are provided: (a) against an abnormally high VSWR, and (b) against an arc which might travel toward the window. A high VSWR might result in internal damage to the tube, and an arc arriving at the window would almost certainly result in window damage which would destroy the vacuum. A microwave circuit is used for the VSWR interlocks; the arc detector uses an optical interlock circuit which would detect an arc in the vicinity of the window. Either of these two circuits will feed a pulse to the fast-turn-off circuits associated with the VA-617 TWT driver. The drive signal supplied to the VA-879 can be reduced 45 db in less than 3 μsec and 80 db in less than 5 μsec. This same circuit can also be used for pulsing the drive.

All waveguide in the Haystack RF system is of oxygen-free high-conductivity copper, with a few exceptions where available components were of aluminum. All high-power lines are of WR-137 size waveguide up to the power splitter which feeds the monopulse horn. This large waveguide was chosen in order to provide a greater margin of safety against voltage breakdown without going to a nonstandard size of transmission line. In the high-power waveguide all flanges are the CPRF type, made from stainless steel, and are used with a copper gasket which has been designed to provide the best possible contact between mated pieces of waveguide. In

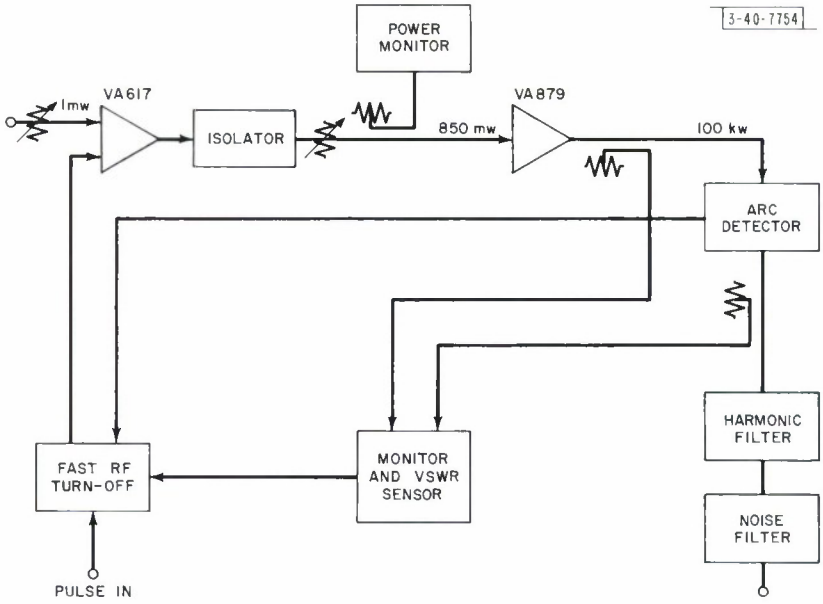

Fig. 36. Transmitter amplifier chain.

resonant-ring tests using this type of flange joint, power levels of over 500 kw CW have been transmitted in WR-137 waveguide without breakdown.

Even with the low loss of WR-137 OFHC copper waveguide (approximately 0.015 db per foot), the ohmic loss in the walls is sufficient to raise the waveguide temperature to intolerable values when 100 kw CW is transmitted. In order to overcome this difficulty, a copper tubing is attached to opposite waveguide walls by means of solder or heat-conducting epoxy mixtures (usually epoxy containing a large amount of powdered metal which has high thermal conductivity), and water is passed through the tubing. This technique reduces the waveguide surface temperature to very nearly the temperature of the cooling fluid.

In the communication mode of operation, where transmission and reception occur simultaneously, there was concern that the second harmonic of the transmitted signal leaking to the receivers might be of sufficient amplitude to impair reception. With the parametric amplifiers being used, the idler frequency is close to the second harmonic of the transmitted signal so that any incoming second harmonic could be supported by the idler circuits and cause possible saturation effects or undesirable modulation products.

A General Electric Company leaky wall filter was procured for use in this mode of operation and was designed to remove the second and all higher harmonics. This filter is water-cooled, as are all the high-power components, and has an insertion loss at the transmitter frequency of 0.1 db. It provides approximately 50 db attenuation at the second harmonic. This unit has been high-power tested and broke down at 200 kw CW.

In order to reduce the interference produced by transmitter-generated noise at the receiving frequency, a high-power noise-rejection filter was designed and a prototype has been built and successfully tested. The rejection band, tuned to the receiver frequency, provides 60 db rejection over an 8-Meps band, while the passband at the receiver frequency has less than 0.03-db loss. Voltage breakdown occurred at 175 kw CW in resonant-ring tests.

The design and construction of a 100-kw CW circulator which would operate over the band of 7700 to 8400 Mcps was contracted to the Raytheon Company. The product was in essence two circulators in parallel. A circulator has been successfully high-power tested to 115 kw CW in a resonant ring. The insertion loss is 0.2 db at 7750 Mcps after temperature stabilization. The cold loss is about 0.28 db.

Most of the low-level microwave circuits are in WR-112 waveguide because of the availability of components at the frequency band of interest. These circuits include the monopulse comparators, all the low-level drive circuits, and the circuits at the input of the receivers. Since all these transmission lines are held to a minimum length, the added loss over that which could be realized with the larger WR-137 guide is negligible.

Two types of receiver protection are required: (a) for radar experiments, when the transmitter will be turned off while receiving, and (b) for communication experiments, when simultaneous transmission and reception will be required. For Venus radar experiments, the times involved are so long that mechanical switches will be used for receiver protection. Waveguide switches with electrically driven actuators have been procured and tested. These provide a minimum of 80 db isolation between the input and the disconnected terminal. It is expected that the circulator and the orthogonal mode transducers will both provide a minimum of 20 db additional isolation so the maximum peak power incident on the receivers should be 10^{-5} watts.

For more conventional radar applications, where the transmitted pulse might be 2 to 5 msec long and the range a few hundred or a few thousand miles, the mechanical switches are much too slow. A gaseous discharge attenuator has been designed which will provide 80 to 100 db of protection. The low-level insertion loss has been measured to be less than 0.05 db when cold. The recovery time is about 300 μsec to the 3-db point and about 450 μsec to complete recovery.

For the communications mode, diplexers have been designed for the purpose of separating the 7750- and 8350-Mcps bands. For early experiments, only the 8350 frequency will be used on reception, so the function of the diplexers is to provide 30 db of transmitter signal rejection in the 8350-Mcps circuits.

Reflection filters for the purpose of reducing the amount of transmitter power leaking to the receiver were procured from Rantec, Inc. The rejection properties of these filters were improved by retuning, so that over 90 db of rejection has been achieved over the transmitter bandwidth. With these improved filters it may be possible to eliminate the diplexers for experiments that do not require reception at the transmitter frequency.

The Haystack antenna employs the Cassegrainian type of microwave optics, fed by a horn located near the vertex of the 120-foot-diameter parabolic reflector. A feed horn has been designed to provide inputs to a monopulse comparator. The system is designed to transmit right-hand circular polarization and receive both senses of circular polarization. Monopulse tracking will be done only with the left-hand circularly polarized received signal.

Figure 37 is a block diagram of the monopulse system. The transmitter power is fed into a four-way power divider, into the orthogonal mode transducers (OMT), through the circular polarizers, and into the multimode horns shown in Fig. 38.

The multimode horn, fed by four square waveguides, consists of several sections: (a) a transition from four waveguides to a large square cross section (this is perhaps the most critical element in the horn structure); (b) a length of straight waveguide of the large square cross section; and (c) a pyramidal horn.

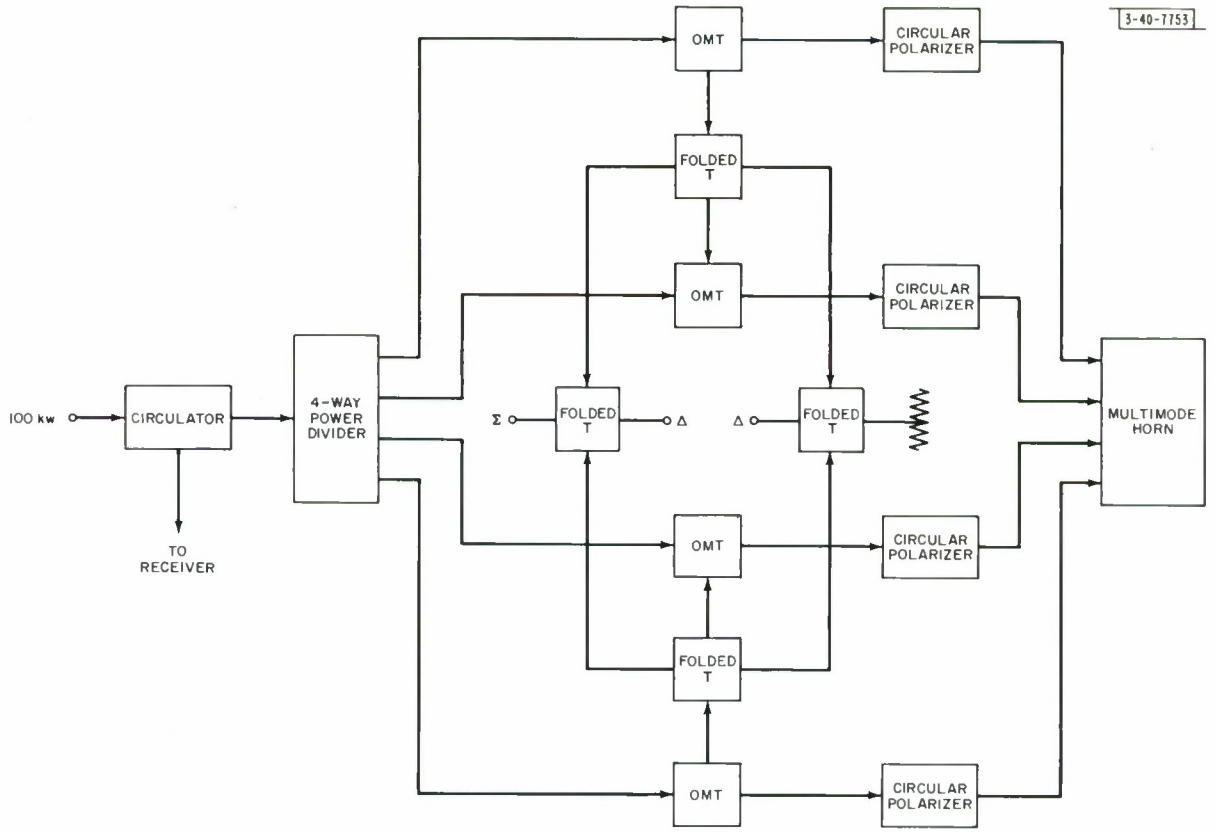

Fig. 37. RF monopulse system.

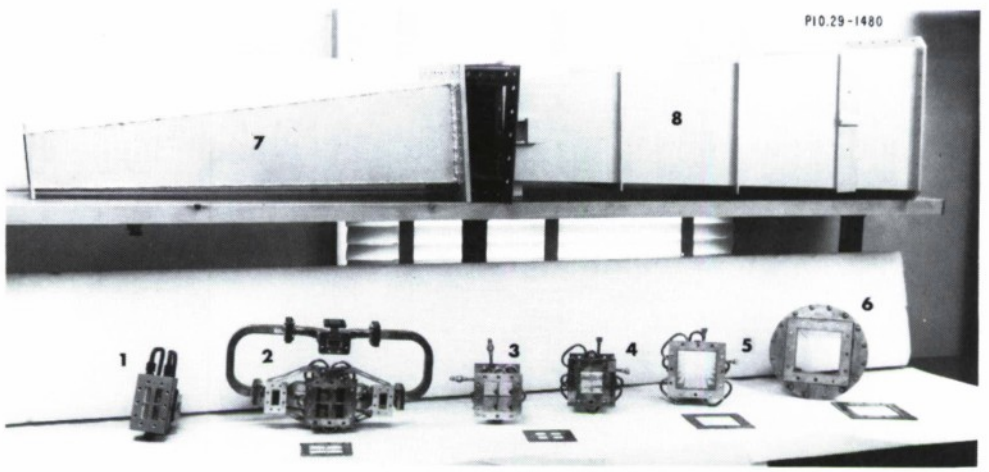

1 4-way power divider
2 Orthogonol mode transducers (4) ond orthogonol mode summing hybrids
3 Circulor polorizer
4 Four-squore-waveguide transition
5 Finned tronsition
6 Straight section
7 Reor horn section (copper)
8 Frant horn section (aluminum)

Fig. 38. Multimode horn subassemblies.

The transition from the four square waveguides to the large square cross section is designed to excite the modes necessary for obtaining angle information and suppressing undesirable modes which may upset the antenna pattern. The transition designed for use in the Haystack antenna achieves this goal. Although not all undesirable modes are completely suppressed, the feed has good patterns in the band 7700 to 8400 Mcps.

The TE_{30} mode is generated by the presence of the short circuit in the aperture plane of the four square waveguides. The configuration of the transition to square waveguide was designed to generate an equal amount of TE_{30} mode out of phase with that generated at the four-waveguide aperture. At the same time, it was necessary to avoid generation of undesirable higher-order TE and TM modes. The fin-loading of the transition accomplishes this.

The feed is well-matched at the transmitter frequency, 7750 Mcps, and has a VSWR of 1.2 at 8350 Mcps corresponding to a reflection loss of less than 0.05 db. Compared with a four-horn monopulse feed, the forward gain of this feed is greater by nearly 1 db over the band of interest. The side lobes of the sum pattern are over 18 db below the main lobe in both planes, compared with 7.5 db and 12.5 db for a four-horn monopulse feed.

The purpose of the straight square waveguide section is to adjust the relative phase of the various modes at the horn aperture. This can be done reasonably well for the principal modes, TE_{10}, TE_{20}, (TE_{11}, TM_{11}) degenerate pair and the (TE_{21}, TM_{21}) degenerate pair. The TE_{10} mode represents the forward or sum signal, and the TE_{20} and (TE_{21}, TM_{21}) degenerate pair form the difference modes. The (TE_{21}, TM_{21}) degenerate pair provides the E-plane taper which makes possible the reduction of E-plane side lobes. The H-plane side lobes are reduced by the elimination of the TE_{30} mode at the horn throat. Typical patterns for the multimode horn are shown in Fig. 39.

The low-noise receivers in the initial high-power plug-in room are two-stage, diode parametric amplifiers capable of being cooled in either liquid nitrogen or liquid helium. Initially,

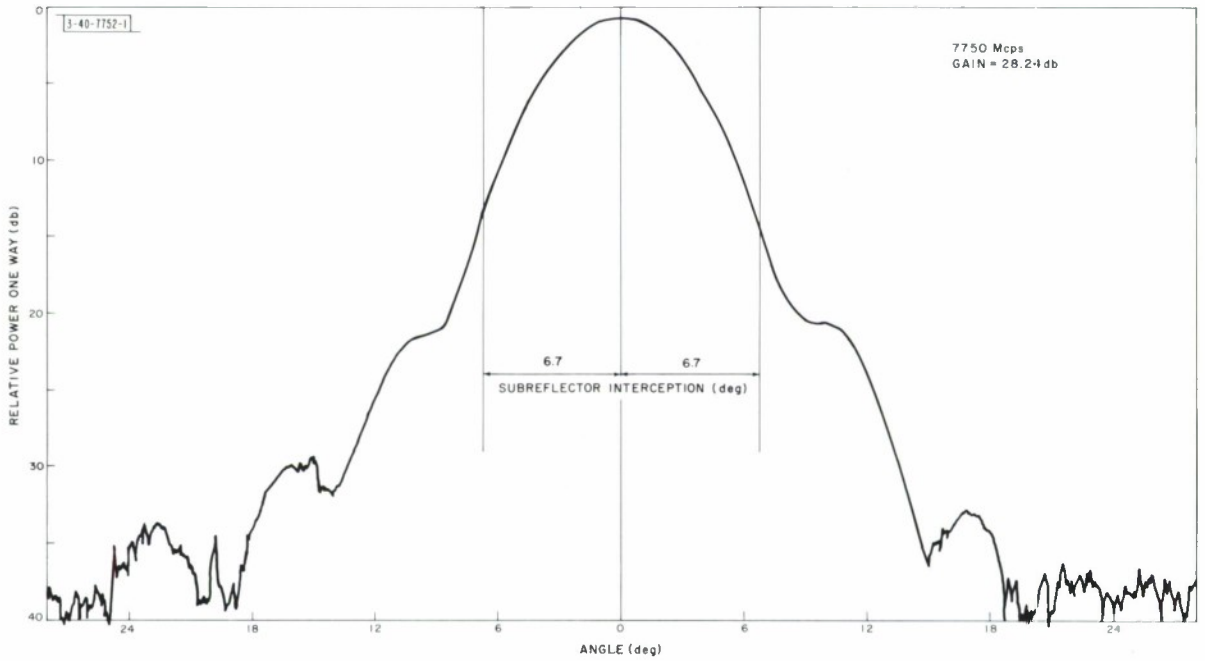

Fig. 39. Typical pattern of multimode horn.

only two channels will be received – the normal circularly polarized return and the orthogonal circularly polarized signal – at either 7750 or 8350 Mcps. Provision has been made for modification of the RF system to include simultaneous reception on up to seven receiving channels at 7750 and/or 8050 and/or 8350 Mcps.

The parametric amplifiers are modified Texas Instruments, Inc. units which were originally designed for room-temperature operation. These units operate in the nondegenerate mode with a pump frequency of 24 Gcps. To insure good amplitude stability, four-port circulators are employed in conjunction with the amplifiers and the pump level is regulated. With 13-db gain per stage, the over-all bandwidth of a cascade at the 3-db points is 40 to 60 Mcps. At this gain the receiver noise temperature is 300 to 330 °K at room temperature, 100 to 125 °K in liquid nitrogen, and 30 to 65 °K in liquid helium. It is anticipated that these amplifiers will eventually be replaced by models with lower heat capacity and improved microwave characteristics.

The initial experiments will be conducted using batch-filled dewars. Units manufactured by Cryenco, Inc. (Fig. 40) have demonstrated ability to hold helium for 10 hours and nitrogen for 3 days. A recently developed dewar using super-insulation held helium for 18 hours. Closed-cycle helium refrigeration systems (Fig. 41) are undergoing evaluation and will be installed at a later date. Provisions are being made for installation of cryostats in the RF box and compressors on the support structure close to the RF box. Such a system should allow continuous operation at liquid helium temperature. The cryostats have been designed to accommodate four two-stage paramps, the four first stages being at liquid helium temperature and the second stages located at an intermediate heat station (approximately 60 °K).

Fig. 40. Two-stage parametric amplifier and dewar to be used in control tests.

Fig. 41. Air Products closed-cycle refrigerator with four 2-stage amplifiers to be used in later tests.

X. AUXILIARY INSTRUMENTATION

Several of the more important supporting subsystems of the Haystack research facility are briefly described in this section. Other standard or commercially available components, such as precision rubidium frequency standards, WWV and loran receivers for frequency comparison, monitor scopes, and recorders, are not described.

A. Real-Time Digital Clock

A digital clock has been constructed which accepts a 100-kcps signal from a frequency standard and produces tuning signals in binary, binary-coded decimal, and decimal words. The binary word is composed of 30 bits with a 100-μsec least-significant bit. The least-significant bits of the binary-coded decimal and decimal words represent 10 μsec of time. The digital clock also contains a real-time pulse generator consisting of ten identical circuits, providing ten independent outputs. Each circuit will allow an operator, through the use of eight decade switches, to select pulses in increments of 1/100 second throughout a 24-hour period. These pulses are available for trigger, monitoring, and display purposes.

B. Range Encoder and Tracker

When the Haystack facility is used in the radar mode, equipment is available for encoding the range of the received signal and for automatically tracking a designated target. This unit encodes the range of a detected radar return in a 25-bit binary register which can accommodate a maximum range of approximately 550,000 nm. When this unit is driven by a 5-Mcps frequency standard, it provides a range resolution of approximately 100 feet. This equipment also provides a tracking gate and a false-alarm gate at a range determined manually or by the computer or the sequential Doppler processor. Manual handwheel control of the tracking-gate width and toggle control of the false-alarm-gate width are provided in all modes of gate position control.

C. Sequential Doppler Processor

A sequential Doppler processor (SDP) has been provided to permit compensation of a frequency shift in a received narrow-bandwidth signal. This compensation is needed to permit efficient detection and to generate an indication of the Doppler shift of an observed target. This equipment accepts a 2000-μsec pulsed-radar target return at a 130-Mcps IF and performs an estimation of the radial velocity of the target based on each individual return. A pulse generated in the SDP following each signal return is used by the range encoder to count the range of the target and to initiate the transfer of the Doppler estimation (a 21-bit binary word) into the Univac 490 computer via the Doppler-interface equipment. The SDP produces an output Doppler word whose least-significant bit represents a return frequency shift of 1 cps (velocity of approximately 0.05 ft/sec at 8 Gcps) for any input frequency shift up to ±750 kcps (approximately ±37,000 ft/sec). It provides single-pulse detection and parameter estimation at input signal-to-noise ratios as low as −20 db. For use by the monopulse processing equipment, the SDP provides a digitally constructed oscillator signal whose frequency is offset from the frequency of the target return by a constant amount which is independent of the Doppler shift of the target.

D. Monopulse Angle Estimator

The monopulse estimator is a "sum and difference" system with amplitude comparison for generation of an absolute error signal and phase comparison for derivation of error sense. Signal normalization in the monopulse circuits is accomplished by using a common amplifier channel with frequency multiplexing. This equipment accepts three 2000-μsec pulsed-radar-target return signals from the 130-Mcps IF amplifiers which represent the sum, azimuth difference, and elevation difference signals at the antenna. These are delayed until a CW signal is received from the SDP to remove the Doppler frequency shift. Then the difference signals are normalized to the sum signal and all three are passed through narrow-band filters to improve the signal-to-noise ratio. The normalized difference analog error signals are used by the antenna drive servos and are digitized (7 bits plus sign for each axis) for use in the Univac 490 computer.

E. Test Signal Generator and Target Simulator

A test signal generator and target simulator has been constructed which will have the following uses:

(1) General-purpose signal source for checking system operation,

(2) Doppler extractor (centers the received Doppler-shifted signal in the IF pass band),

(3) Monopulse system tester (entire tracking loop),

(4) Computer-controlled target simulator (R, $\dot{R}$, angle error, amplitude).

The output of the system is an X-band signal shifted by any amount up to 2 Mcps. This RF signal will be derived from the 5-Mcps system standard and will have a very high stability. The output will also be capable of being pulse-modulated with pulse lengths from 1 μsec to infinity (CW). The output power from the simulator will be controlled by a precision attenuator so that sensitivity checks can be made in the system receiver. Independent phase and amplitude control of the signals sent to the error channels of the monopulse receiver will also be provided so the tracking system can be controlled by the simulator. All the variable parameters in the system will be capable of either manual or computer (Univac 490) control.

XI. CONTOUR-MONITORING INTERFEROMETER

As the orientation of the antenna and the ambient temperature in the radome change, the reflector surface will be displaced from an ideal parabolic contour. A novel radio-frequency interferometric technique has been devised to permit monitoring the displacement of selected points on the reflector surface while it is in normal use. In this monitoring system, radio-frequency phase measurements are used to observe changes in the path length between selected target locations on the reflector surface and a test unit located near the secondary reflector. To isolate the signals reflected from the selected target location from the signals that are reflected from surrounding parts of the structures, special modulated targets are employed.

Figure 42 is a block diagram of the antenna contour-monitoring equipment. The system may be divided into four main parts: (a) the microwave transmitter and receiver, (b) the modulated targets, (c) frequency-conversion equipment, and (d) the contour-deviation indicator.

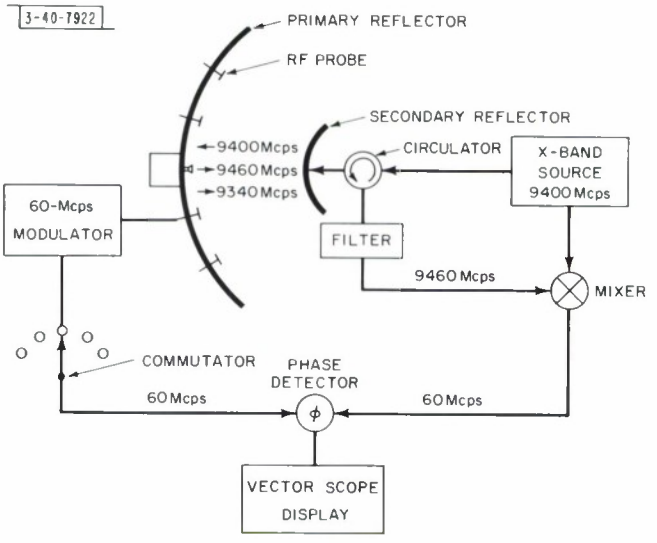

Fig. 42. Block diagram of contour-monitoring equipment.

The feed horn on the stable microwave source radiates a CW 9.46-Gcps signal toward the main reflector. At selected points on this reflector, special pickup elements are located. Each of these special targets, mounted on the reflector, consists of a small antenna horn or elemental array with dimensions of approximately 3 inches × 3 inches. The small pickup antenna elements are normally terminated by a matched resistive load. Upon application of an externally applied signal, the impedance of the matched load can be changed so that nearly all the energy falling on the target will be reflected. A 60-Mcps signal is used to modulate the impedance of the antenna element. The modulated signal reflected from a target beats with the transmitter signal and generates ±60-Mcps modulation components on the 9.46-Gcps carrier. The receiver selects the lower sideband component of this composite signal and translates it to a 60-Mcps IF signal. The phase of the modulation of this 60-Mcps signal is dependent upon the two-way path distance between the radiating horn and the test element at the reflector.

For convenience, a test instrument called a vector scope, which has been developed for monitoring television signals, has been modified for use in this application. Since the vector scope is designed to accept a 3.58-Mcps signal, frequency conversion equipment is used to translate the 60 Mcps to 3.58 Mcps. The vector scope also produces the 60-Mcps signal that is used for modulating the diodes in each target. This 60-Mcps signal is phase coherent with the 3.58-Mcps reference signal.

The display on the vector scope is a spot on the face of a cathode-ray tube which is displaced by an angle corresponding to the phase angle between the 3.58-Mcps reference signal and the converted 3.58-Mcps received signal. Because of the coherence of the frequency-conversion equipment, this angle is also a measure of the phase angle between the received 60-Mcps signal and the original 60-Mcps modulation. Deviations of the target on the reflector surface will show up as angular motion of the dot on the indicator.

An electronic switch is used to sequentially distribute the 60-Mcps modulation signal to the various targets. The preset delays are adjusted to give a display on the vector scope in which the location of the dot for each target corresponds to its physical location on the surface of the antenna.

A calibration channel is provided to correct for phase changes in the receiver. This is done by injecting a modulation signal into the receiver and using the output of the vector scope phase detector to adjust a calibration delay that is common to all the target modulation lines.

A more precise measure of target deviation may be obtained by operating the vector scope in a null mode. This would be particularly useful for the precise observation of deviations of a single target as the antenna is positioned through all attitudes.

In 1963, a breadboard version of this system was tested on an antenna range. With the transmitter and target separated by 25 feet, a 0.005-inch motion of the target was readily detected. Target displacements of 0.100 inch were measured with an accuracy better than ±0.005 inch with a transmitter power of 500 milliwatts. The measurement accuracy was nearly as good with only 15 milliwatts of transmitter power.

These and other tests helped point out some possible design changes to improve the system. For example, the possibility of trading off transmitter power for antenna aperture is a desirable feature of the single-sideband receiving system. Since the bandpass filter will reject the carrier by some 50 db, it could be possible to increase the transmitter to a level of several watts without transmitter leakage becoming a problem. Some directivity must be maintained in the test antennas in order that supporting struts may be kept out of the transmission path.

The RF interferometer monitoring system has not yet been installed on the Haystack antenna, but this should be accomplished within the next few months. The microwave components for the transmitter and receiver will be located at the secondary reflector. To minimize weight and to increase reliability, only solid state active elements have been employed. A crystal oscillator followed by a varactor multiplier chain is being used to provide a very stable (1 part in 10^7) lightweight microwave source. A temperature-compensated cavity filter is used to reject the carrier and upper sideband by 50 db while attenuating the desired lower sideband by only 1.5 db. It is intended that the vector scope and frequency-conversion equipment will be located at ground level in the Haystack control room. This system will provide an independent technique for cross checking the deflectional behavior of the reflector with that obtained from optical measurements.

XII. STATUS AND FUTURE PLANS

At the present time, all the major elements of the Haystack system are installed at the Tyngsboro site, and integration tests are under way. The mechanical test program on the antenna has been completed, and preliminary pattern measurements have been taken at 8 Gcps. These pattern measurements indicate that the beamwidth and sidelobe structure of the antenna are in good agreement with theoretical estimates. A comprehensive calibration program to determine the antenna gain and system temperature at 8 Gcps, 15 Gcps, and 35 Gcps will be started shortly.

In recent weeks, additional test data on the antenna have been analyzed. These data show that the FRAN deflection computations are in close agreement with measured data and indicate that the analytic solution is even more exact than the best optical surveying instrumentation that can be devised for field use. It is now possible to utilize actual contour antenna survey data in conjunction with FRAN calculations to obtain plots of the antenna surface contour for various elevation orientations. Two typical plots are shown in Figs. 43(a) and (b).

Contour information of this type has been used in a computer program to compute the antenna gain and sidelobe levels under a variety of conditions. Based on these computer runs, it

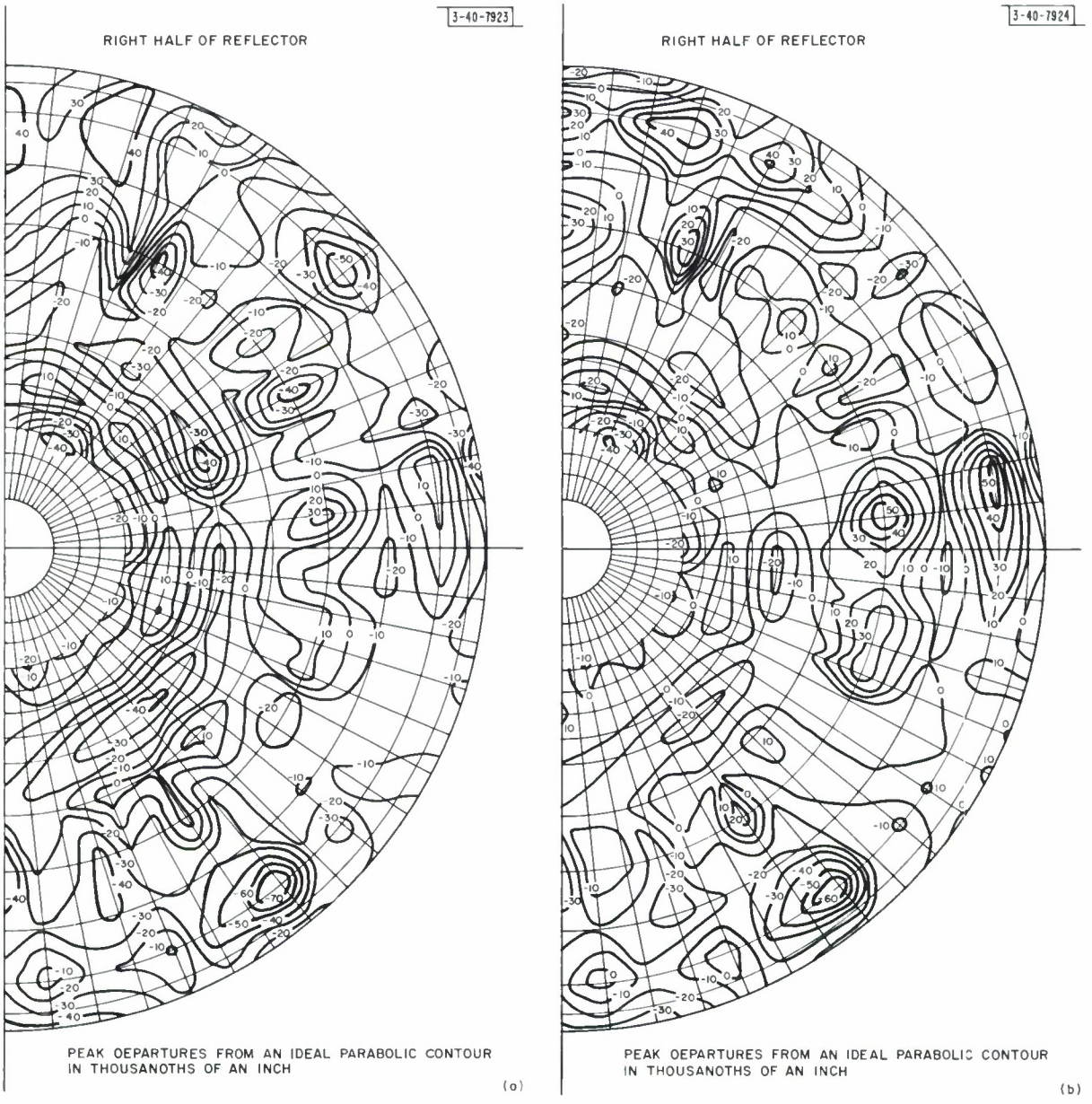

Fig. 43. Peak deviations of reflector surface, as rigged 14 May 1964, calculated from face-up survey data plus calculated gravity effects (nominal temperature environment). (a) 30° elevation angle; (b) 60° elevation angle.

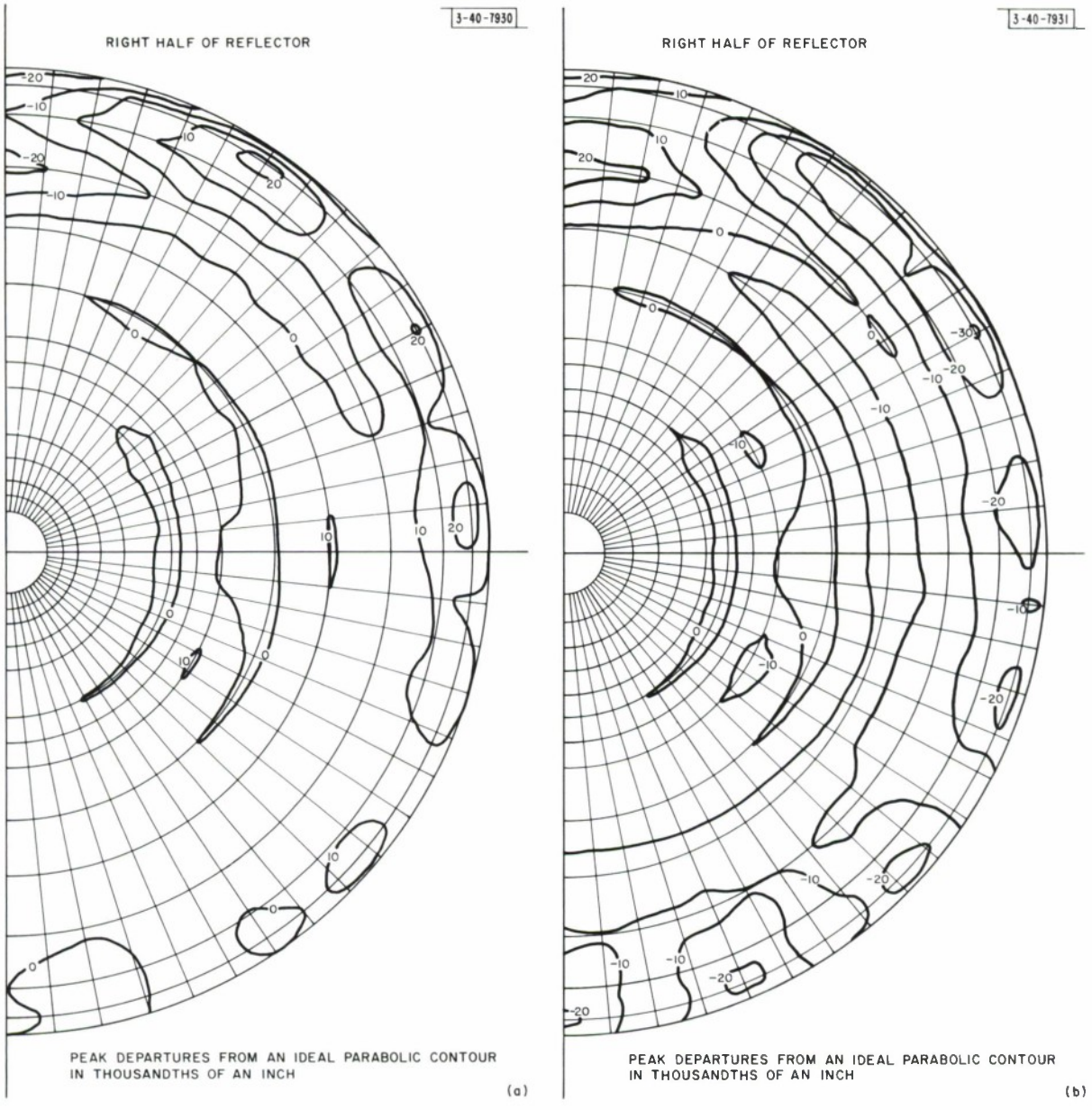

Fig. 44. Computed surfoce contour ofter ponel reodjustments. Does not include opproximotely 0.007-inch error due to opticol instrumentotion ond locol ponel errors. (o) 30° elevotion ongle; (b) 60° elevotion ongle.

is now possible to predict that the antenna gain should be within 2 db of an ideal antenna at 35 Gcps. The major residual contour errors are attributable to surveying and panel adjustment inaccuracies.

Because the reflector panels were made with such great care, and because there now is a very complete understanding of the behavior of the antenna, it is interesting to speculate about the surface contour which could possibly be obtained if the antenna panels were more carefully adjusted. To make this effort worth while, the optical equipment would first have to be recalibrated to minimize residual errors and the thermal gradients within the radome would have to be minimized through the use of air-moving equipment. Figures 44(a) and (b) are plots based on calculations, which show the surface contours that should exist at 30° and 60° elevation angles, respectively, if the antenna surface were readjusted to have minimum distortion at a 45° elevation angle. In addition to the errors in Fig. 44, local contour errors in the panels and measurement system errors would contribute an additional uncertainty of about 0.007 inch. If all appropriate steps were taken, it appears that the electrical performance of the antenna should be quite acceptable at frequencies above 35 Gcps.

It is now evident that the present radome will have a more pronounced effect upon the antenna gain at millimeter wavelengths than will the reflector itself. This is shown in Fig. 45, where the 0.020-inch tolerance curve is representative of the Haystack antenna at the present time (at 45° elevation), and the 0.015-inch tolerance should apply after another phase of instrument calibration and surface adjustment.

For about a year, a Lincoln Laboratory committee has been planning an experimental program for the Haystack facility. The high angular resolution, large effective area and high power of this system offer new capabilities to the experimenter, and many different users will avail themselves of the antenna during the coming year. The installation is well suited to multiple-user operations, and the digital computer control system should make it possible to utilize the available operating time efficiently.

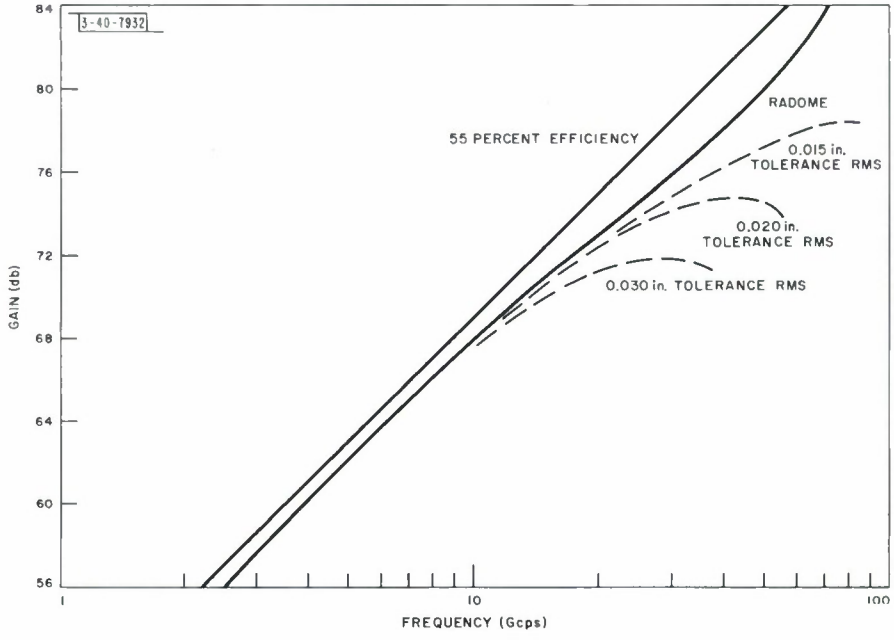

Fig. 45. Estimated gain of antenna in radome for several values of surface tolerance.

P10.29-565A

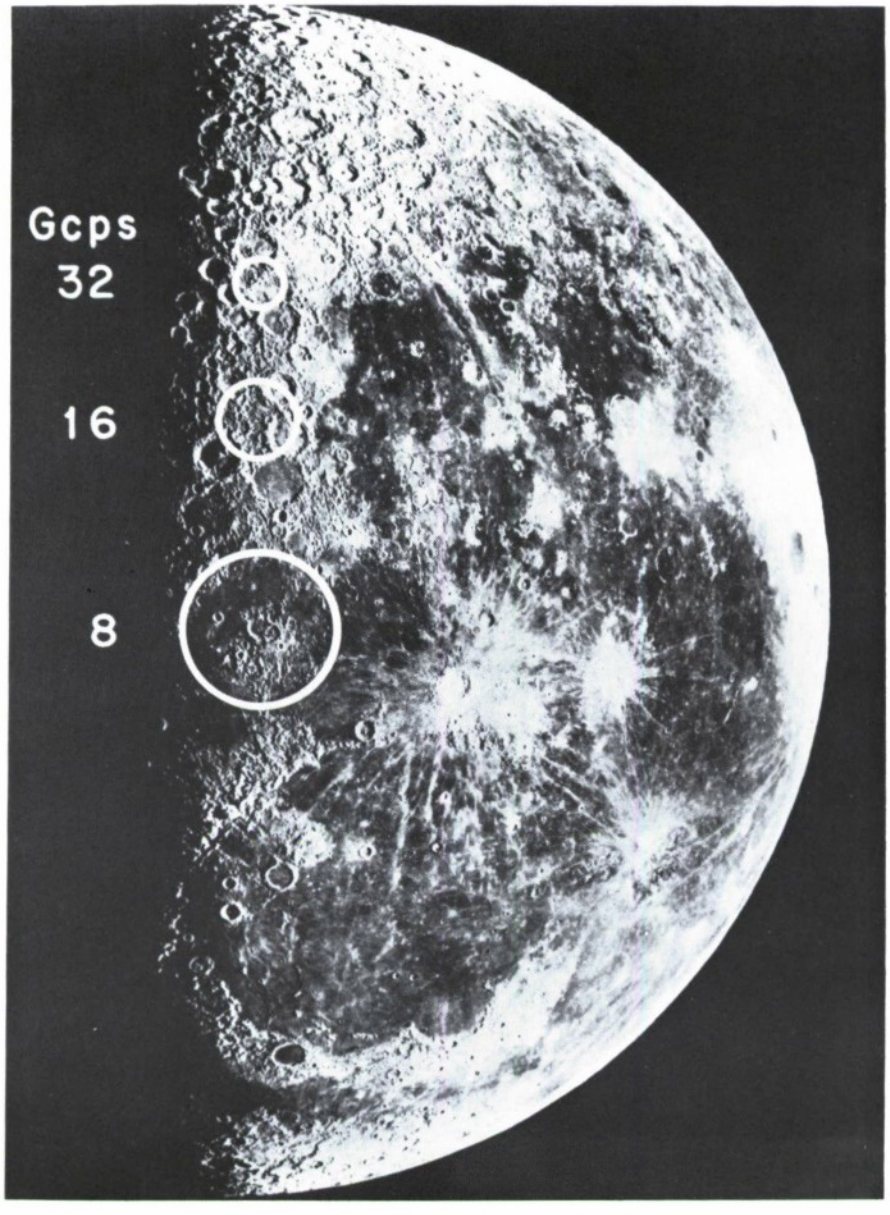

Fig. 46. Half-power antenna beamwidth at 8, 16, and 32 Gcps.

One of the paramount programs which will be conducted throughout 1965 will be to explore the potential usefulness of a very-high-gain ground terminal for space communications. These studies will initially be carried out near 8 Gcps, so that coast-to-coast experiments may be conducted in conjunction with the Project West Ford site near Camp Parks, California. Communication experiments utilizing the moon, Echo-type balloons, the West Ford dipole belt, and other passive reflectors will receive early attention. Communication tests with a small mobile terminal will also be initiated. The Haystack system will also be used to explore the effects of the atmosphere and weather upon microwave communications at 8 Gcps and at higher frequencies. When appropriate satellites are in orbit with microwave transponders, the Haystack terminal will be available for transmission tests.

In the radar mode, the Haystack system will be employed to obtain high-resolution measurements of the moon, Venus, and other planetary objects. Strong radar echoes from the planet Venus should be detectable for many months of the year, and the increased system sensitivity should permit improved measurements. The system should be capable of obtaining radar backscatter echoes from a medium-sized satellite at a range of 20,000 miles and will be able to detect very small targets at ranges of several thousand miles.

The Haystack antenna will also be used for radio astronomy studies at wavelengths throughout the 1.4- to 35-Gcps region of the spectrum. Because of the high resolution of the antenna, it should be possible to map celestial radio sources with unprecedented precision. Figure 46 shows the half-power beamwidth of the antenna at three different frequencies superimposed on the surface of the moon.

BIBLIOGRAPHY

A. R. Dion, "Investigation of Effects of Surface Deviations on Haystack Radiation Patterns," Technical Report 324, Lincoln Laboratory, M.I.T. (29 July 1963), DDC 418740.

A. O. Kuhnel, "Haystack Antenna System Status Report," Technical Report 328, Lincoln Laboratory, M.I.T. (13 September 1963), DDC 600930.

A. A. Galvin, "A Sequential Detection System for the Processing of Radar Returns," Proc. IRE 49, 1417 (1961).

L. D. Massey, "Computer Programs for Haystack Servo Testing," Group Report 1964-38, Lincoln Laboratory, M.I.T. (21 July 1964), DDC 603794, H-598.

H. E. Frachtman, "Haystack Pointing System: Sun," Group Report 1964-40, Lincoln Laboratory, M.I.T. (29 July 1964), DDC 603318, H-596.

P. D. Smith, "Haystack Pointing System: Digital Equipment Organization," to be published.

A. A. Mathiasen and J. D. Drinan, "Haystack Pointing System: Computer Program Structure," to be published.

H. Simpson, "Structural Aspects of Large Precision Antennas," NEREM Record 4, 70 (1962).

H. G. Weiss, "The Haystack Experimental Facility," NEREM Record 4, 108 (1962).

T. F. King and L. P. Farnsworth, "Mechanical Design of a 150-Foot Diameter Metal Space Frame Radome," Paper 59-A-271, Proceedings of the American Society of Mechanical Engineers, November 1959.

G. R. Carroll, "A Hydrostatic Bearing for Haystack," Paper 62-W-299, American Society of Mechanical Engineers Winter Meeting, November 1962.

J. Banche and D. N. Ulry, "Axial Load Design for High Performance Radar Antenna Structures," Paper 62-WA-302, American Society of Mechanical Engineers Winter Meeting, November 1962.

H. Simpson and J. Antebi, "Space Frame Analysis and Applications to Other Types of Structures," Proceedings of the First Annual Workshop of SHARE Design Automation Committee, 24-26 June 1964.

ACKNOWLEDGMENTS

The planning, design, installation, and testing of this new facility has been successful only because of the hard work, competence and diverse talents of a large number of individuals and organizations. It is not feasible to enumerate the contributions made by each participant in the program during its four-year history, and it is hoped that those individuals whose names are not listed below will obtain appropriate recognition in future reports.

Sponsor

United States Air Force
480L Program Office
Electronic Systems Division
L.G. Hanscom Field
Bedford, Massachusetts
AF Project Officer:
Lieutenant John Shock

Principal Contractors

Antenna:
North American Aviation, Inc.
Columbus (Ohio) Division
G. Guise, R.R. Howard, J. Banche,
G.R. Carroll, J. Doyle, J. Rutledge

Transmitter:
Energy Systems, Inc.
Palo Alto, California
E. Altschul

Computer:
Univac Division
Sperry Rand Corporation
St. Paul, Minnesota

Radome:
H.I. Thompson Fiber Glass Company
Gardena, California

Lincoln Laboratory Staff

Antenna:
Structural
P.L.E. Alherti (now deceased),
W.R. Fanning, F.A. Folino, P. Stetson,
E.W. Blaisdell, F.G. DeSantis

Bearing and Control
A.O. Kuhnel

Cable Wrap and Cabling
M.L. Stone, E.W. Blaisdell,
L.P. Rainville

RF Box Installations
M.W. Brawn, E.A. Chateauneuf,
C.A. Peterson, A.M. Rich

Site Development
D.C. Moore, J.B. Paddleford,
C.T. Frerichs

Optical Measurements
D.G. Stuart

RF Configuration
L.J. Ricardi

Antenna (continued):
Performance Calculations
J. Ruze

Radome:
Design
J.A. Vitale, A. Cohen, T.F. King,
R.A. Muldoon, J.F. Orabona

Performance Calculations
J. Ruze

Transmitter:
G.L. Guernsey, S.J. Miller,
M.L. Stone, M.H. Leavy

Receiver:
R.P. Ingalls, G.M. Hyde,
C.M. Steinmetz, E. Gehrels,

Communications Equipment Room:
Transmitter
C.W. Jones, A.F. Standing, W.A. Both,
W.A. Andrews, C.A. Peterson

Receiver
C. Blake, L.W. Bowles

System Integration
J.S. Arthur, M.L. Stone

Antenna Feed
K.J. Keeping

Radiometer System:
S. Weinreb, M.L. Meeks

Pointing and Control System:
F.E. Heart, A.A. Mathiasen, D.R. Bromaghim,
P.D. Smith, J.S. Arthur, J.D. Drinan,
P. Stylos, H.E. Frachtman, W.R. Crowther,
R. Teoste, S.B. Russell, J.E. Gillis

Range and Doppler Tracking Equipment:
A.A. Galvin, D.R. Bromaghim,
W.H. Drury, W.F. Kelley

Contour-Monitoring Interferometer:
L.W. Bowles

Consultants

Structural Design:
H. Simpson
Simpson, Gumpertz and Heger, Inc.
Cambridge, Massachusetts

Hydrostatic Bearing:
Prof. D. Fuller
Civil Engineering Department
Columbia University
New York, New York

My task as the Lincoln Laboratory Haystack project engineer has been aided substantially by the following members of the Laboratory Staff: P.L.E. Alberti, A.O. Kuhnel, F.A. Folino, J.S. Arthur, M.L. Stone, and A.A. Galvin. The major contributions of P.L.E. Alherti, prior to his tragic death in an automobile accident in June 1964, will long be remembered by his associates. Special credit is also due Lieutenant John Shock, the AF Project Officer, R.R. Howard of the NAA engineering department, J. Doyle, the NAA site supervisor, and H. Simpson, consultant, for their major contributions to the antenna program.

Security Classification

DOCUMENT CONTROL DATA - R&D

(Security classification of title, body of abstract and indexing annotation must be entered when the overall report is classified)

1. ORIGINATING ACTIVITY *(Corporate author)*

Lincoln Labs.,
Lexington, Mass.

2a. REPORT SECURITY CLASSIFICATION

UNCLASSIFIED

2b. GROUP

N/A

3. REPORT TITLE

The Haystack Experimental Facility

4. DESCRIPTIVE NOTES *(Type of report and inclusive dates)*

Technical Report

5. AUTHOR(S) *(Last name, first name, initial)*

Weiss, H.G.

6. REPORT DATE	7a. TOTAL NO. OF PAGES	7b. NO. OF REFS
Sept 64	61	0

8a. CONTRACT OR GRANT NO.	9a. ORIGINATOR'S REPORT NUMBER(S)
b. PROJECT NO. AF19(628)500	TR-365
c.	9b. OTHER REPORT NO(S) *(Any other numbers that may be assigned this report)* ESD-TDR-64-378
d.	

10. AVAILABILITY/LIMITATION NOTICES

Qualified Requesters May Obtain From DDC.
Aval From OTS.

11. SUPPLEMENTARY NOTES	12. SPONSORING MILITARY ACTIVITY
	ESD, L.G. Hanscom Field, Bedford, Mass.

13. ABSTRACT

A New ground station for space communications, radar and radio astronomy research has recently been completed at Tyngsboro, Massachusetts. This installation, which is named Haystack, employs a 120-foot-diameter fully Steerable antenna enclosed in a metal space-frame radome. Advanced design and construction techniques have been developed to achieve a reflector with a very precise parabolic contour. The antenna will operate very efficiently at wavelengths of 3 cm and will also provide a useful capability at wavelengths as short as 8 mm. The antenna incorporates a "plug-in" equipment room behind the reflector which makes it possible to conveniently utilize the antenna for a variety of both active and passive experiments. At the highest operating frequency, the half-power width of the antenna beam will be less than 0.02°. To provide appropriate control for this very narrow antenna beam, a general-purpose digital computer has been integrated into the facility. The RF configuration of the antenna is compatible with the use of high-power transmitters and cooled, low-noise receiving equipment. A versatile 1-Mw average power, high-voltage supply has been provided for energizing transmitting equipment. This new installation will provide a unique capability in the microwave portion of the spectrum for communications, radar and radio astronomy.

DD FORM 1 JAN 64 1473

Security Classification

14. KEY WORDS	LINK A		LINK B		LINK C	
	ROLE	WT	ROLE	WT	ROLE	WT
Communications Equipment Radar Antenna Parabalic Antenna Radome Performance Tests Experimental Data Design Computer (Univac 490) (IBM 7094) Radiometers Tracking Doppler Systems Data Processing Systems						

INSTRUCTIONS

1. ORIGINATING ACTIVITY: Enter the name and addresa of the contractor, aubcontractor, grantee, Department of Defense activity or other organization *(corporate author)* lasuing the report.

2a. REPORT SECURITY CLASSIFICATION: Enter the overall security classification of the report. Indicate whether "Restricted Data" is included. Marking is to be in accordance with appropriate security regulationa.

2b. GROUP: Automatic downgrading ia specified in DoD Directive 5200.10 and Armed Forces Industrial Manual. Enter the group number. Also, when applicable, show that optional markings have been used for Group 3 and Group 4 as authorized.

3. REPORT TITLE: Enter the complete report title in all capital lettera. Titles in all casea ahould be unclassified. If a meaningful title cannot be selected without classification, show title clasaification in all capitals in parenthesia immediately following the title.

4. DESCRIPTIVE NOTES: If appropriate, enter the type of report, e.g., interim, progress, summary, annual, or final. Give the incluaive dates when a specific reporting period la covered.

5. AUTHOR(S): Enter the name(s) of author(s) as shown on or in the report. Enter last name, first name, middle initial. If military, show rank and branch of service. The name of the principal author is an absolute minimum requirement.

6. REPORT DATE: Enter the date of the report as day, month, year; or month, year. If more than one date appears on the report, uae date of publication.

7a. TOTAL NUMBER OF PAGES: The total page count should follow normal pagination procedures, i.e., enter the number of pages containing information.

7b. NUMBER OF REFERENCES: Enter the total number of references cited in the report.

8a. CONTRACT OR GRANT NUMBER: If appropriate, enter the applicable number of the contract or grant under which the report was written.

8b, 8c, & 8d. PROJECT NUMBER: Enter the appropriate military department identification, such as project number, subproject number, system numbers, task number, etc.

9a. ORIGINATOR'S REPORT NUMBER(S): Enter the official report number by which the document will be identified and controlled by the originating activity. Thia number must be unique to this report.

9b. OTHER REPORT NUMBER(S): If the report has been assigned any other report numbers *(either by the originator or by the sponsor)*, also enter this number(s).

10. AVAILABILITY/LIMITATION NOTICES: Enter any limitations on further dissemination of the report, other than those imposed by security classification, using atandard atatementa such as:

(1) "Qualified requestera may obtain copies of thia report from DDC."

(2) "Foreign announcement and diaaemination of this report by DDC is not authorized."

(3) "U. S. Government agencies may obtain copies of this report directly from DDC. Other qualified DDC usera shall request through

_____."

(4) "U. S. military agencies may obtain copies of this report directly from DDC. Other qualified usera ahall request through

_____."

(5) "All distribution of this report is controlled. Qualified DDC users shall request through

_____."

If the report has been furniahed to the Office of Technical Services, Department of Commerce, for sale to the public, indicate this fact and enter the price, if known.

11. SUPPLEMENTARY NOTES: Use for additional explanatory notes.

12. SPONSORING MILITARY ACTIVITY: Enter the name of the departmental project office or laboratory sponsoring *(paying for)* the research and development. Include address.

13. ABSTRACT: Enter an abstract giving a brief and factual summary of the document indicative of the report, even though it may also appear elsewhere in the body of the technical report. If additional space is required, a continuation sheet shall be attached.

It is highly desirable that the abstract of classified reporta be unclassified. Each paragraph of the abstract shall end with an indication of the military security classification of the information in the paragraph, represented as *(TS), (S), (C), or (U)*.

There is no limitation on the length of the abstract. However, the suggested length is from 150 to 225 words.

14. KEY WORDS: Key words are technically meaningful terms or short phrases that characterize a report and may be used as index entries for cataloging the report. Key words must be selected so that no security classification is required. Identifiers, such as equipment model designation, trade name, military project code name, geographic location, may be used as key words but will be followed by an indication of technical context. The assignment of links, rules, and weights is optional